MODULE 2.6.2 PHARMACOLOGY WRITTEN SUMMARY

FDA-CBER-2021-5683-0708843

TABLE OF CONTENTS

FDA-CBER-2021-5683-0708844

LIST OF TABLES

LIST OF FIGURES

LIST OF ABBREVIATIONS

Abbreviation	Term
ACE2	angiotensin converting enzyme 2
BAL	Bronchoalveolar lavage
CDC	Centers for Disease Control
COVID-19	Coronavirus disease 2019
CT	Cytoplasmic tail
DART	Developmental and reproductive toxicology
dLIA	Direct Luminex immunoassay
DSPC	1,2-distearoyl-*sn*-glycero-3-phosphocholine
ELISA	enzyme-linked immunosorbent assay
ELISpot	Enzyme-linked immunospot
FITC	Fluorescein isothiocyanate
FP	Fusion peptide
GD	Gestation day
GFP	Green fluorescent protein
GMC	Geometric mean concentration
GMT	Geometric mean titer
HCS	Human convalescent sera
HR	Heptad repeat
HRP	Horseradish peroxidase
ICOS	inducible costimulatory molecule
ICS	Intracellular cytokine staining
IFA	immunofluorescence
IFN	Interferon
IgG	Immunoglobulin G
IL	interleukin
IM	intramuscular
IN	Intranasal
IT	intratracheal
kDa	kilodalton
LD	Lactation day
LLOQ	lower limit of quantification
mAb	Monoclonal antibody
MERS	Middle East respiratory syndrome
mL	milliliter
mNG	mNeongreen
modRNA	Modified mRNA
MW	molecular weight
NHP	Nonhuman primate
ORF	Open reading frame
P2 S	stable prefusion S including two proline substitutions
PBS	Phosphate-buffered saline
PD	Protease domain

Abbreviation	Term
PFU	Plaque forming unit
PND	Postnatal day
PVDF	Polyvinylidene fluoride
pVNT	Pseudotype neutralization titer
$pVNT_{50}$	50% pseudovirus neutralizing titer
$pVNT_{90}$	90% pseudovirus neutralizing titer
RNA	ribonucleic acid
RDRP	RNA-dependent RNA polymerase
RT-qPCR	Reverse transcription-quantitative polymerase chain reaction
S	SARS-CoV-2 spike glycoprotein
S1 / S2	SARS-CoV-2 spike glycoprotein subdomains 1 / 2
S2′	S2 protease cleavage site
SARS-CoV-2	severe acute respiratory syndrome coronavirus 2
SDS-PAGE	Sodium dodecyl sulfate-polyacrylamide electrophoresis
SEC	Size exclusion chromatography
SS	Signal sequence
Tfh	T follicular helper cell
TLR	Toll-like receptor
TM	transmembrane
TNF	tumor necrosis factor
μg	microgram
ULOQ	Upper limit of quantification
US	United States
USA	United States of America
VEE	Venezuelan equine encephalitis virus
VSV	Vesicular stomatitis virus
VNT_{50}	50% virus neutralizing titer
WHO	World Health Organization

FDA-CBER-2021-5683-0708848

2.6.2. PHARMACOLOGY WRITTEN SUMMARY

2.6.2.1. Introduction

BNT162b2 (BioNTech code number BNT162, Pfizer code number PF-07302048) is BNT162b2 (V9), a nucleoside-modified mRNA (modRNA) vaccine that encodes the SARS-CoV-2 full-length spike glycoprotein (S). In some preclinical research, a different variant of BNT162b2 was used: BNT162b2 (V8), which has a different codon optimization but encodes a protein with the same amino acid sequence as BNT162b2 (V9). In this document, "BNT162b2" refers to BNT162b2 (V9), unless otherwise specified. The glycoprotein encoded by both BNT162b2 variants includes two amino acid substitutions to proline (P2 S) locking the transmembrane protein in an antigenically optimal prefusion conformation (Pallesen et al, 2017; Wrapp et al, 2020).

The RNA is formulated with functional and structural lipids, which protect the RNA from degradation and enable transfection of the RNA into host cells after IM injection. The formulation contains two functional lipids, ALC-0315 and ALC-0159, and, two structural lipids, DSPC (1,2-distearoyl-*sn*-glycero-3-phosphocholine) and cholesterol.

The modRNA comprises a single-stranded, 5′-capped mRNA that is translated upon entering the cell. In addition to the open reading frame (ORF) encoding the SARS-CoV-2 P2 S antigen, each modRNA contains common structural elements optimized for high translational efficacy of the RNA. ModRNA also contains a substitution of 1-methyl-pseudouridine for uridine. This substitution decreases recognition of the vaccine RNA by innate immune sensors, such as toll-like receptors (TLRs) 7 and 8, resulting in decreased innate immune activation and increased protein translation (Kariko et al, 2005). Vaccination with modRNA is characterized by the strong expansion of Th1-skewed antigen-specific T follicular helper (Tfh) cells, which stimulate and expand germinal center B cells, thereby resulting in particularly strong, long-lived, high-affinity antibody responses (Sahin et al, 2014; Pardi et al, 2018). The structural elements of BNT162b2 contain non-coding sequences optimized for prolonged and strong translation of the P2 S antigen-encoding RNA component.

2.6.2.2. SARS-CoV-2 S as a Vaccine Target

SARS-CoV-2 is an enveloped, positive sense, single-stranded RNA virus that is coated with S, which gives the virion its characteristic corona or "crown" appearance (Figure 2.6.2-1). Coronavirus S is a major target of virus neutralizing antibodies and is a key antigen for vaccine development. S is a transmembrane glycoprotein responsible for receptor recognition, attachment to the cell, and viral envelope fusion with a host cell membrane resulting in genome release, which is driven by the S conformation change leading to the fusion of viral and host cell membranes. For infection, S requires proteolytic cleavage by two host proteases, a furin-like protease between the S1 and S2 subunits, and by the serine protease TMPRSS2 at a conserved site directly preceding the fusion peptide (S2') (Figure 2.6.2-2; Bestle et al, 2020; Hoffmann et al, 2020). While the membrane-proximal S2 furin cleavage fragment is responsible for membrane fusion, the membrane-distal S1 fragment, with its receptor-binding domain (RBD), recognizes the host receptor and binds to the target host cell. SARS-CoV S and SARS-CoV-2 S have similar structural properties and

FDA-CBER-2021-5683-0708849

bind to the same host cell receptor, angiotensin converting enzyme 2 (ACE2)
(Zhou et al,2020).

Figure 2.6.2-1. Replication Cycle of a Coronavirus
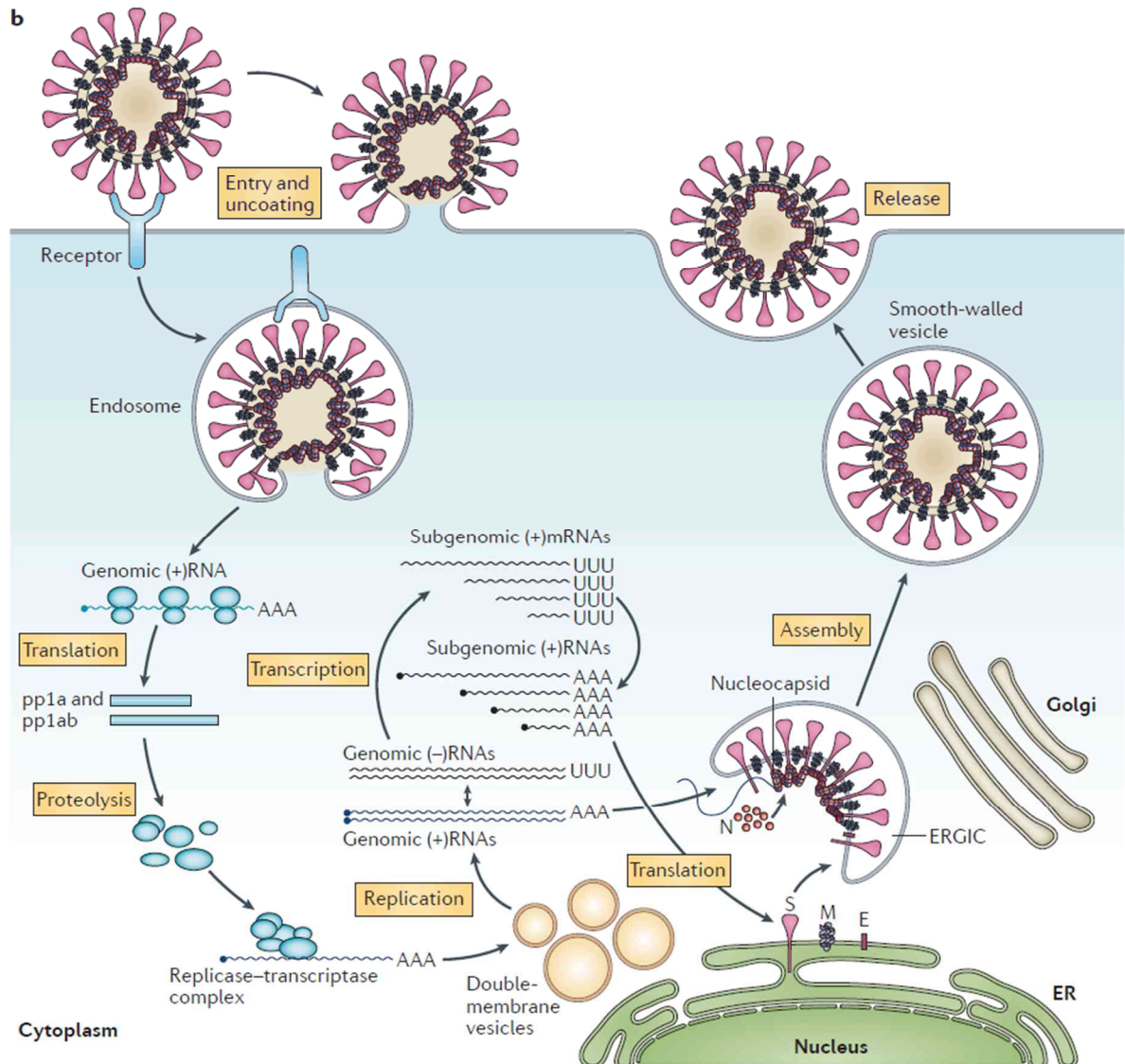
Source: de Wit et al, 2016

S is a large, trimeric glycoprotein that exists predominantly in a prefusion conformation on the virion (Ke et al, 2020). Spontaneously and during cell entry, the S1 fragment dissociates, and the S2 fragment undergoes a fold-back rearrangement to the post-fusion conformation in a process that facilitates fusion of viral and host cell membranes. S is critical for the induction of virus neutralizing antibodies by the host immune system (Zakhartchouk et al, 2007; Yong et al, 2019). Some monoclonal antibodies against S, particularly those directed against the RBD, neutralize SARS-CoV and Middle East respiratory syndrome (MERS)-CoV infection *in vitro* and *in vivo* (Hulswit et al, 2016). Vaccines targeting the S protein are sufficient to induce strong neutralizing immune responses (Al-Amri et al, 2017).

FDA-CBER-2021-5683-0708850

The RBD forms membrane distal "heads" on the S trimer that are connected to the body by a hinge. In the native S, the RBD alternates between an open (up) and closed (down) position. Although potent neutralizing epitopes have been described when the RBD is in the "heads down" closed conformation, the "heads up" receptor accessible conformation exposes a potentially greater breadth of neutralizing antibody targets (Brouwer et al, 2020; Liu et al, 2020; Robbiani et al, 2020). A P2 mutant (P2 S) variant of S contains two consecutive prolines introduced at amino acid positions 986 and 987, between the central helix (CH) and heptad repeat 1 (HR1) (Figure 2.6.2-2). These mutations lock S in the prefusion conformation (Pallesen et al, 2017; Wrapp et al, 2020). A proportion of P2 S has one RBD in the "heads up" and two RBDs in the "heads down" position, and there is probably a dynamic equilibrium as the heads hinge up and down (Cai et al, 2020; Henderson et al, 2020).

Figure 2.6.2-2.   Schematic of the Organization of the SARS-CoV-2 S Glycoprotein
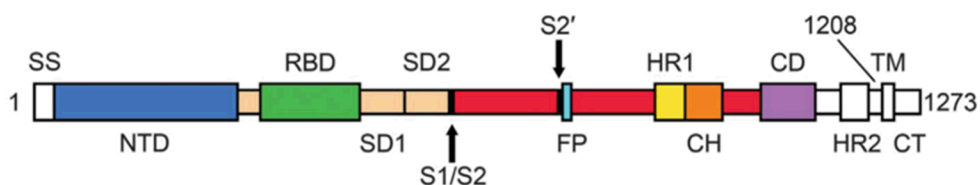
The S1 furin cleavage fragment includes the signal sequence (SS), the N terminal domain (NTD), the receptor binding domain (RBD, which binds the human cellular receptor, ACE-2), subdomain 1 (SD1), and subdomain 2 (SD2). The furin cleavage site (S1/S2) separates S1 from the S2 fragment, which contains the S2 protease cleavage site (S2′) followed by a fusion peptide (FP), heptad repeats (HR1 and HR2), a central helix (CH) domain, the connector domain (CD), the transmembrane domain (TM) and a cytoplasmic tail (CT).
Source: modified from Wrapp et al, 2020.

BNT162b2 (V9) encodes for a full-length P2 S. The V9 codon optimization variant contains a higher content of cytosine ribonucleotides than V8 for increased protein expression and is the focus of this marketing application. The RNA-expressed P2 S is membrane anchored. It elicits of a potent humoral neutralizing antibody response and Th1-type CD4$^+$ and CD8$^+$ cellular response to block virus infection and kill virus infected cells, respectively.

2.6.2.3. In Vitro Expression of Antigens from BNT162b2 (V9) RNA

Different in vitro methods were performed to analyze SARS-CoV-2 P2 S expression. To assess transfection frequencies in cells exposed to BNT162b2 RNA mixed with a commercial transfection reagent or exposed to BNT162b2 (which is LNP-formulated), flow cytometry analysis was performed. Immunofluorescence staining of transfected cells was used to assess cellular localization.

Flow cytometry analysis of HEK293T cells transfected with either BNT162b2 RNA or LNP-formulated BNT162b2 led to high frequencies of cells being transfected, with BNT162b2-transfected cells being transfected at a slightly higher frequency than cells exposed to BNT162b2 RNA mixed with a commercial transfection reagent (Figure 2.6.2-3).

FDA-CBER-2021-5683-0708851

There were no differences in cell viability after transfection with BNT162b2 RNA or BNT162b2 compared to non-transfected cells. Furthermore, co-localization of the S protein antigen with an ER marker was detected by immunofluorescence experiments in HEK293T cells expressing BNT162b2-RNA suggesting the S protein is processed within the ER (Figure 2.6.2-4).

Figure 2.6.2-3.   Flow Cytometry Analysis of BNT162b2 Transfection Frequency
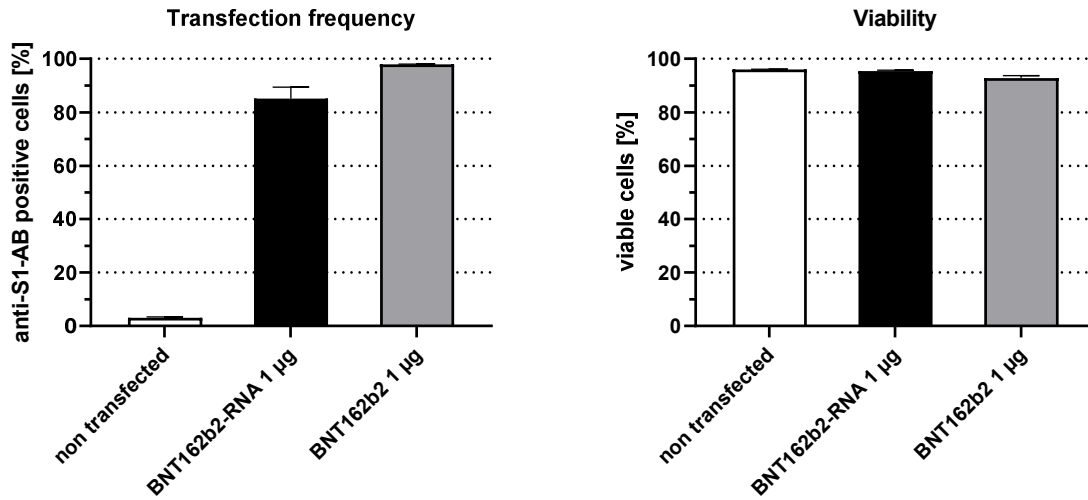
HEK 293T cells were transfected using RiboJuice™ mRNA transfection reagent (Merck Millipore) with 1 μg of the RNA encoding BNT162b2 P2 S (V9) (BNT162b2 RNA) or the BNT162b2 (LNP-formulated RNA). After 18 h in culture, cells were stained with a viability dye, fixed, permeabilized and stained with a monoclonal rabbit antibody recognizing S1 and labelled with AlexaFluor647. Non-transfected cells were used as a control.

FDA-CBER-2021-5683-0708852

Figure 2.6.2-4.   Immunofluorescence Detection of P2 S in BNT162b2 Transfected Cells
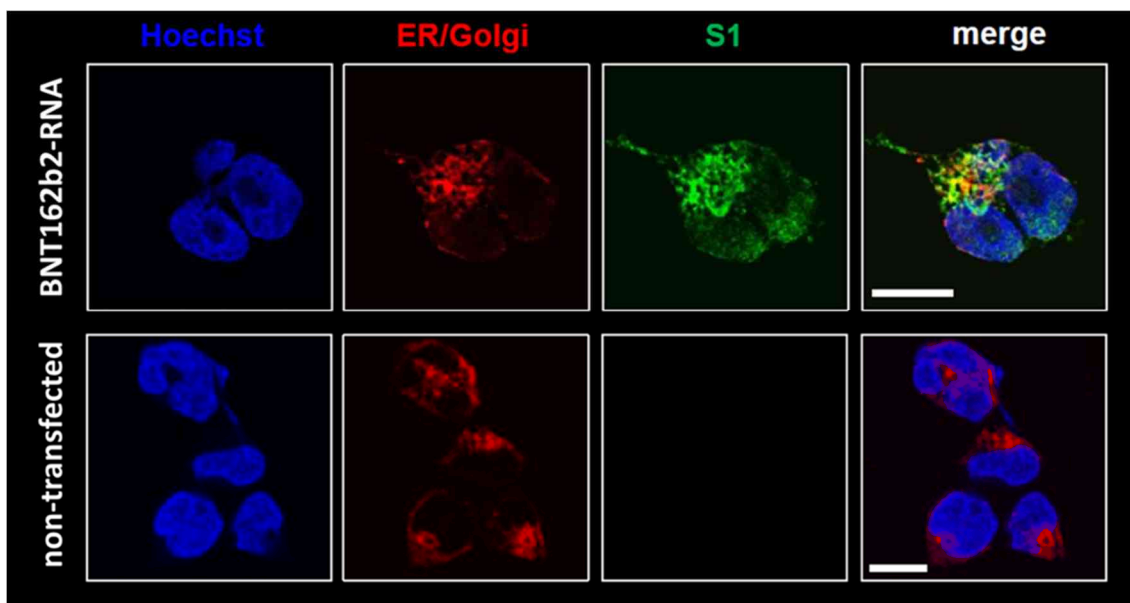
HEK293T cells were transfected with BNT162b2 (V9) RNA using RiboJuice™ RNA transfection reagent (Merck Millipore). After 18 h in culture, cells were fixed, permeabilized and stained for DNA to visualize the nucleus with Hoechst (blue), for the endoplasmic reticulum and Golgi (ER/ Golgi) with concanavalin A and Golgi tracker, both Alexa Fluor™ 594 conjugated (red). Cells were stained for P2 S with a monoclonal anti-S1 antibody and Alexa Fluor® 488 (green). The merged color panels show that the P2 S expressed by BNT162b2 (V9) colocalizes with the ER/ Golgi marker (scale: 10 µm). A control of non-transfected cells is shown in the lower row.

2.6.2.4. Structural and Biophysical Characterization of P2 S as a Vaccine Antigen

For structural characterization, P2 S was expressed in Expi293F cells from DNA that encodes the same amino acid sequence as BNT162b2 RNA, with the addition of a C-terminal TwinStrep tag for affinity purification (VR-VTR-10741). To confirm surface expression of untagged P2 S as well as the ability of P2 S to bind to human ACE2, flow cytometry experiments were performed on nonpermeabilized cells (Figure 2.6.2-5). Antibodies to the RBD, S1, and S2 were pre-incubated with Alexa-488 anti-IgG Fab for staining, and a nucleic acid dye was used to separate live and dead cells. To confirm binding of human ACE2, P2 S-expressing cells were labeled with the extracellular domain of human ACE2 pre-incubated with a FITC-labeled antibody against an affinity tag on the ACE2. Finally, anti-RBD human neutralizing antibodies B38 and H4 isolated from a COVID-19 convalescent patient (Wu et al, 2020) as well as the anti-RBD therapeutic antibody CR3022 (Yuan et al, 2020) were similarly confirmed to bind the surface-expressed P2 S.

FDA-CBER-2021-5683-0708853

Figure 2.6.2-5.   Binding to Cell Surface-Expressed Recombinant P2 S
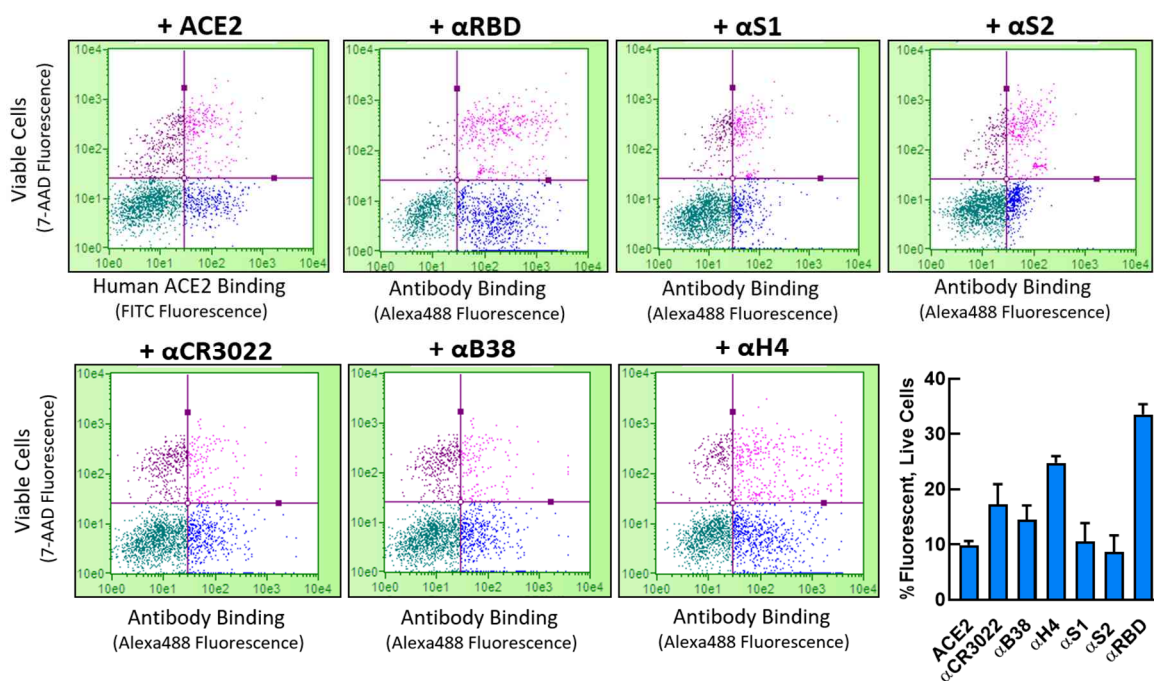
P2 S antigen was over-expressed in Expi293F cells, and surface expression confirmed by staining with antibodies against the RBD, S1, and S2 regions of the full-length S protein. Human ACE2 extracellular domain (ACE2) as well as the therapeutic antibody CR3022 and two neutralizing antibodies isolated from a COVID-19 convalescent patient, B38 and H4, were further confirmed to bind to surface express P2 S. The nucleic acid dye 7-AAD was used identify viable cells (lower quadrants in flow plots). Binding to surface expressed P2 S over background in live cells is quantified across replicates in the bar graph.

Purification of the recombinant P2 S was based on a procedure described previously (Cai et al, 2020), with minor modifications. Upon cell lysis, P2 S was solubilized in 1% NP-40 detergent. The TwinStrep-tagged protein was then captured with StrepTactin Sepharose HP resin in 0.5% NP-40. P2 S was further purified by size-exclusion chromatography and eluted as three distinct peaks in 0.02 % NP-40 as previously reported (Cai et al, 2020). Protein from the first peak of a size exclusion column, containing intact P2 S and dissociated S1 and S2, was assayed by biolayer interferometry (Figure 2.6.2-6). The trimeric P2 S bound to the human ACE2 peptidase domain (ACE2-PD), and an anti-RBD human neutralizing antibody B38 with high affinity (apparent K_D = 1 nM).

FDA-CBER-2021-5683-0708854

Figure 2.6.2-6.   Biolayer Interferometry Sensorgrams for Binding of P2 S to ACE2-PD and B38 mAb
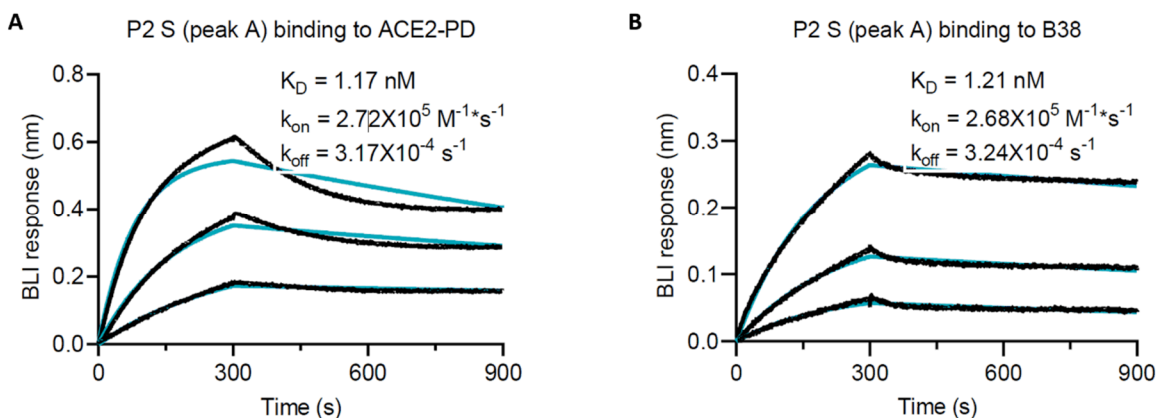
P2 S with a C-terminal TwinStrep tag expressed in Expi293F cells, was detergent solubilized and purified by affinity and size exclusion chromatography. Protein from the first peak of a size exclusion column, containing intact P2 S and dissociated S1 and S2, was assayed by biolayer interferometry on an Octet RED384 (FortéBio) at 25 °C in running buffer consisting of 25 mM Tris pH 7.5, 150 mM NaCl, 1mM EDTA and 0.02 % NP-40. Sensorgrams showing the binding kinetics of TwinStrep-tagged P2 S to immobilized **A**, human ACE2-PD and **B**, B38 monoclonal antibody. The highest concentration tested for P2 S was 71 nM with 2 more 3-fold dilutions. The binding curves were globally fit to a 1:1 Langmuir binding model with R^2 values greater than 0.95. Actual binding data (black) and the best fit of the data to a 1:1 binding model (green). Apparent kinetic parameters are provided in the graphs.

Purified TwinStrep-tagged P2 S was characterized structurally using cryo-electron microscopy (cryoEM). 2D classification of particles from cryoEM data revealed a particle population that closely resembles the prefusion conformation of SARS-CoV-2 spike protein (Figure 2.6.2-7A). Processing and refinement of this dataset yielded a high-quality 3D map with a nominal resolution of 3.29 Å (Figure 2.6.2-7B), into which a previously published atomic model (PDB ID: 6VSB) was fitted and rebuilt. The rebuilt model shows good agreement with reported structures of prefusion full-length wild type S (Cai et al, 2020) and its ectodomain with P2 mutations (Wrapp et al, 2020). Three-dimensional classification of the dataset (Figure 2.6.2-7C) showed a class of particles that was in the one RBD 'up' (accessible for receptor binding), two RBD 'down" (closed) conformation and represented 20.4% of the trimeric molecules. The remainder were in the all RBD 'down' conformation. The RBD in the 'up' conformation was less well resolved than other parts of the structure, suggesting conformational flexibility and a dynamic equilibrium between RBD 'up' and RBD 'down' states as also suggested by others (Cai et al, 2020; Henderson et al, 2020).

The well-resolved trimeric prefusion structure and the high affinity binding to ACE2 and human neutralizing antibodies demonstrate that the recombinant P2 S authentically presents the ACE2 binding site and other epitopes targeted by many SARS-CoV-2 neutralizing antibodies.

Figure 2.6.2-7.   CryoEM P2 S Structure at 3.29 Å Resolution
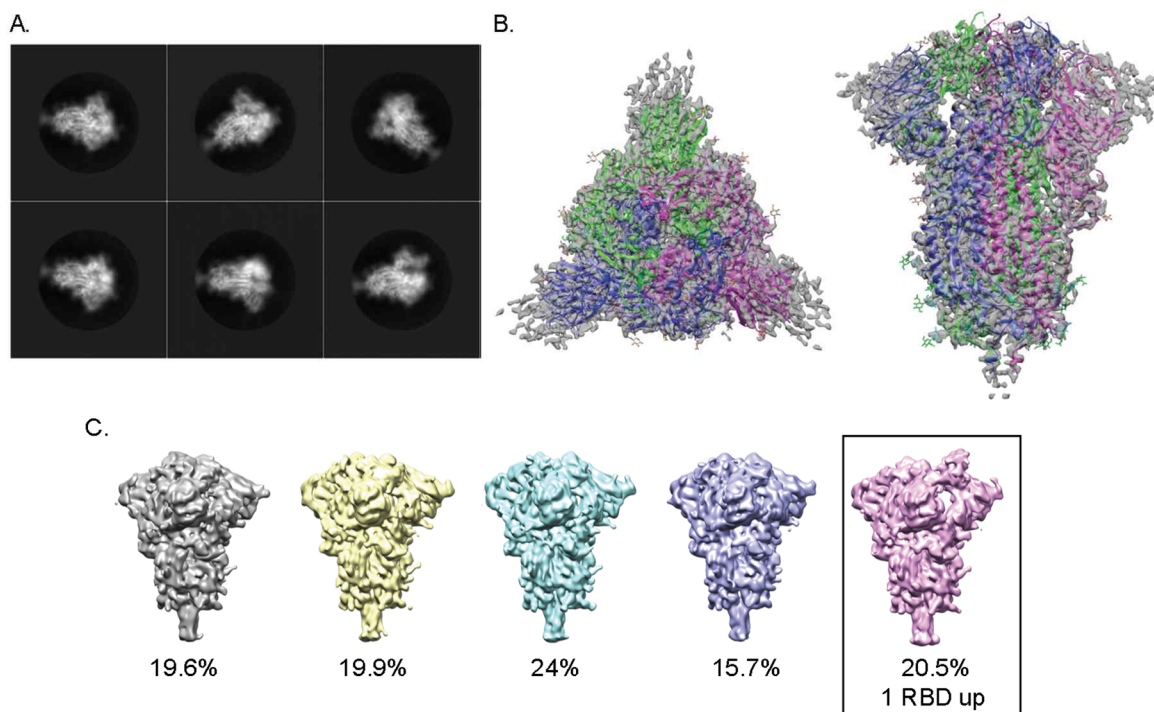
A. 2D class averages of TwinStrep-tagged P2 S particles extracted from cryoEM micrographs. Box size is 39.2 nm in each dimension. **B**. 3.29 Å cryoEM map of TwinStrep-tagged P2 S, with fitted atomic model, showing top (perpendicular to the three-fold axis) and side (parallel to the three-fold axis) views. CryoEM model is based on PDB 6VSB and was fitted into the structure using manual rebuilding in Coot and real-space refinement in Phenix. ~28,000 micrographs were collected using a Titan Krios electron microscope operating at 300 kV accelerating voltage, and image processing and 3D reconstructions were performed using Warp and RELION. **C**. Maps of P2 S produced by 3D classification indicate some heterogeneity in positioning of the RBD domains. Percentages of the particle population represented in each class are indicated below the models.

2.6.2.5. Immunogenicity of BNT162b2 (V9) in Mice

The immunogenicity of BNT162b2 (V9) in mice was investigated (Report R-20-0085).

Four groups of eight female Balb/c mice were immunized on day 0 with 0.2 µg, 1 µg or 5 µg RNA/animal of BNT162b2, or with buffer alone (control group). Blood was collected on Days 7, 14, 21 and 28 after immunization to analyze the antibody response by SARS-CoV2- RBD or S1 IgG ELISA and pseudotype neutralization (pVNT) (detailed methods described in Section 2.6.2.12.1 for ELISA and Section 2.6.2.12.2 for pVNT). Binding kinetics of SARS-CoV-2 S1- and RBD-specific IgGs were determined with sera generated at Day 28.

Immunization with BNT162b2 induced IgGs that bind S1 and RBD, while these antibodies were not detected in samples from buffer control animals. A dose-dependent increase in S1-binding IgGs was observed. Antibody concentrations in the serum samples were calculated using a mouse IgG monoclonal standard, and the kinetics of IgGs against S1 and

FDA-CBER-2021-5683-0708856

RBD are shown in Figure 2.6.2-8. At Day 28, the differences in concentrations of IgGs against S1 and RBD in the test groups compared to the buffer control group were statistically significant (S1: p = 0.0259 for 0.2 µg, p < 0.0001 for 1 µg and 5 µg; RBD: p = 0.0072 for 0.2 µg, p < 0.0001 for 1 µg and 5 µg) .

Figure 2.6.2-8.   Anti-S IgG Response 7, 14, 21, and 28 d after Immunization with BNT162b2
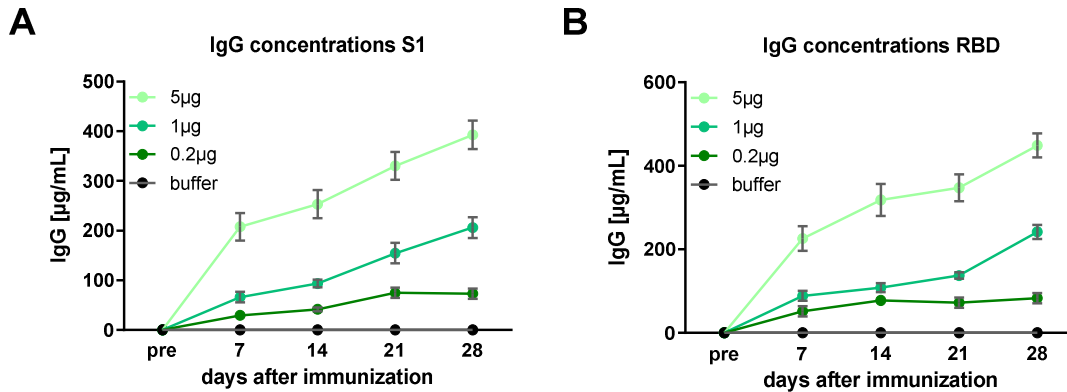
BALB/c mice were immunized IM once with 0.2, 1 and 5 µg BNT162b2 or buffer. On 7, 14, 21, and 28 days after immunization, animals were bled. For individual ΔOD values, the antibody concentrations in the serum samples were calculated. The serum samples were tested by ELISA against (A) recombinant S1 and (B) recombinant RBD. Group mean antibody concentrations are shown (±SEM). Group size n=8. Statistical significance of the differences in IgG concentrations between the test groups and the control group was assessed by one-way ANOVA test with Dunnett's multiple comparison post-test on day 28.

At Day 28 after immunization, vaccine-elicited IgG against the S1 domain showed a very strong binding affinity (geometric mean KD 12 nM) including IgG binding the RBD with high affinity (geometric mean KD 0.99 nM), both with high on-rate (geometric mean kon: 3.33 x 104/Ms for S1-specific affinity; 6.02 x 105/Ms for RBD-specific affinity) and low off-rate (geometric mean koff: 4.00 x 10-4/s for S1-specific affinity; 5.97 x 10-4/s for RBD-specific affinity) (Figure 2.6.2-9).

FDA-CBER-2021-5683-0708857

Figure 2.6.2-9.   Binding Kinetics of Murine SARS-CoV-2 S1- and RBD-specific IgGs
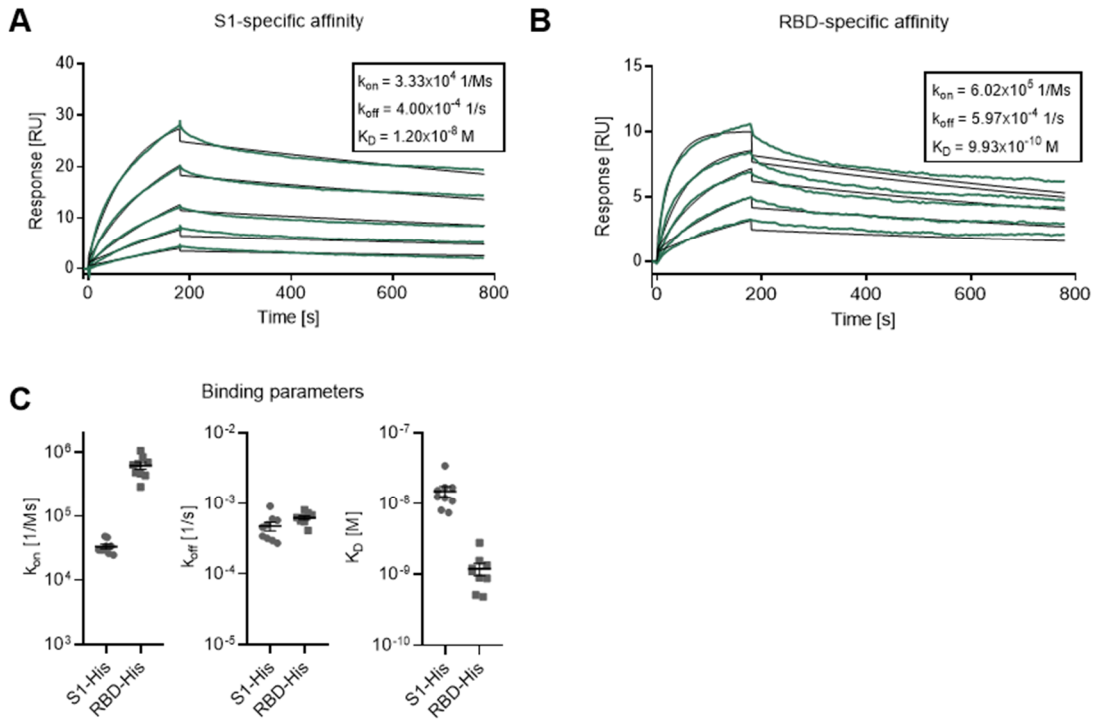
BALB/c mice were immunized IM once with 5 µg BNT162b2. On Day 28 after immunization, animals were bled. IgG in the sera were tested for binding to recombinant histidine-tagged S1 (A) or recombinant histidine tagged RBD (B) (Sino Biological) using surface plasmon resonance spectroscopy in multi-cycle mode with concentrations ranging from 25-400 nM (S1-His) or 1.562-50 nM (RBD-His). Binding kinetics were calculated using a global kinetic fit to a 1:1 Langmuir model. Binding parameters are given in (C). Actual binding data (black) and the best fit of the data to a 1:1 binding model (green). One point in the graphs stands for one mouse. Group size n=8. Mean ± SEM is shown by horizontal bars with whiskers for each group.

In pVNT analysis, dose-dependent increases in neutralizing antibodies were observed (Figure 2.6.2-10).

Figure 2.6.2-10.   BNT162b2 Pseudovirus Neutralizing Titers 14, 21, and 28 d after Immunization
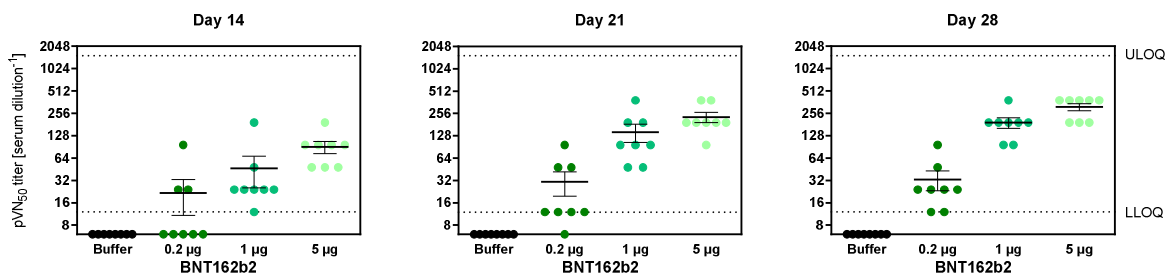
BALB/c mice were immunized IM once with 0.2, 1 and 5 µg BNT162b2 or buffer. On 14, 21, and 28 d after immunization, animals were bled. The sera were tested for SARS-CoV-2 pseudovirus neutralization. Graphs depict $pVNT_{50}$ serum dilutions (50% reduction of infectious events, compared to positive controls without serum). One point in the graphs stands for one mouse. Every mouse sample was measured in duplicate. Group size n=8. Mean ± SEM is shown by horizontal bars with whiskers for each group. LLOQ, lower limit of quantification. ULOQ, upper limit of quantification.

The summary of antibody titers on Day 28 is as follows:

Table 2.6.2-1. Summary of IgG Concentrations at Day 28 Post Immunization

	BNT162b2 0.2 µg	BNT162b2 1 µg	BNT162b2 5 µg
Anti S1 total IgG [µg/mL]	73.0 ± 10.4	205.9 ± 21.0	392.7 ± 28.9
Anti RBD total IgG [µg/mL]	83.1 ± 12.3	241.7 ± 17.2	448.6 ± 28.6
pVN_{50} titer [reciprocal dilution]	33.0 ± 9.8	192.0 ± 31.4	312.0 ± 35.1

In addition, the cellular immune response was analyzed. At Day 28 after one immunization, mice were sacrificed and splenocytes were isolated to test for IFNγ release after antigen stimulation by ELISpot. Stimulation of fresh splenocytes with an S-specific overlapping peptide pool induced IFNγ responses in T cells of immunized animals. Splenocytes of the groups immunized with BNT162b2 had significantly higher spot numbers than splenocytes from the groups that received buffer control (Figure 2.6.2-11). To identify the T-cell subtype, an additional ELISpot analysis was performed after separation of fresh CD4^{+} and CD8^{+} cells by MACS isolation from splenocytes obtained from the group immunized with 5 µg BNT162b2. Both CD4^{+} and CD8^{+} cells displayed IFNγ responses.

FDA-CBER-2021-5683-0708859

Figure 2.6.2-11.   ELISpot Analysis Using Splenocytes Obtained on Day 28 after One Immunization
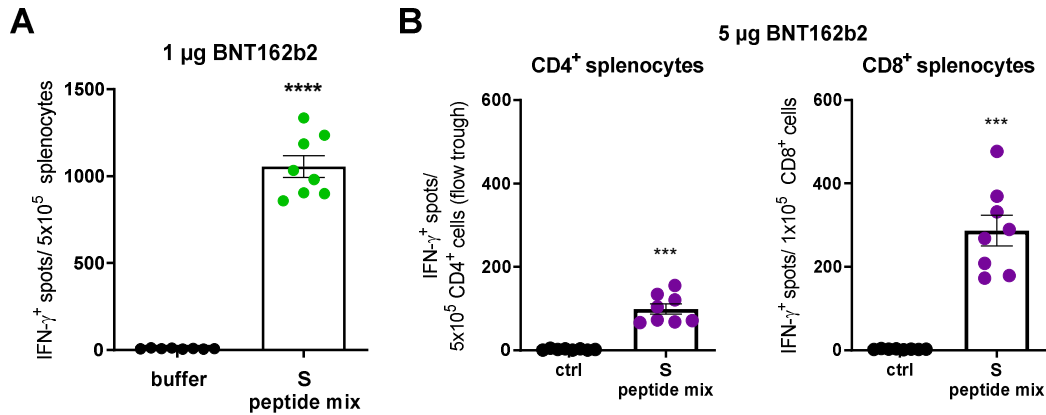
ELISpot assay was performed using (A) bulk splenocytes isolated on Day 28 after IM immunization of mice with 1 µg BNT162b2 or (B) CD4+ and CD8+ splenocytes after magnetic cell separation from the 5 µg BNT162b2 immunized group. Splenocytes were stimulated with S-specific overlapping peptide pools, buffer or an irrelevant control peptide (ctrl), and IFN-γ secretion was measured to assess S-specific T-cell number. Individual spot counts are shown by dots; group mean values are indicated by bars (±SEM). P-values were determined by one-way ANOVA analysis followed by Dunnett's multiple comparisons test. *** $p < 0.001$, **** $p < 0.0001$.

Furthermore, cytokine release data from the S-peptide mix stimulated splenocytes was acquired 28 days after immunization with 5 µg BNT162b2. High levels of the Th1 cytokines IFNγ and IL-2 but minute amounts of the Th2 cytokines IL-4, IL-5 and IL-13 in multiplex immunoassays were detected (Figure 2.6.2-12).

FDA-CBER-2021-5683-0708860

Figure 2.6.2-12. Cytokine Release Analysis Using Splenocytes Obtained on Day 28 after One Immunization
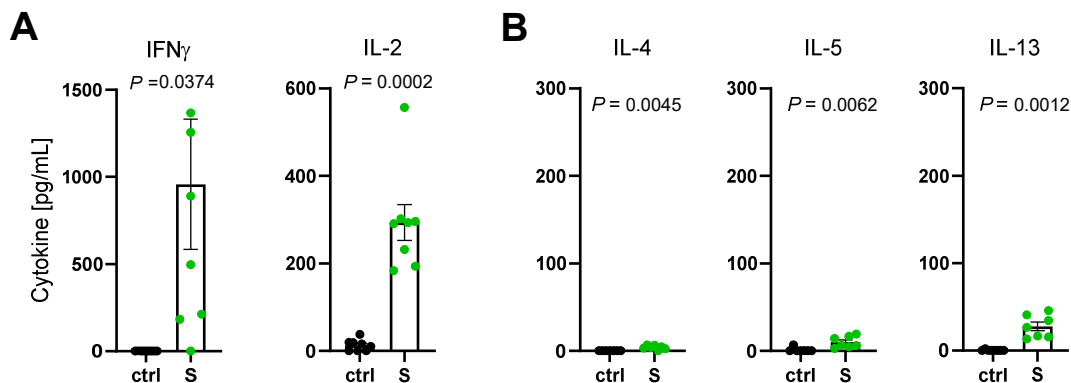
Splenocytes of BALB/c mice immunized IM with 1 µg BNT162b2 were stimulated *ex vivo* with full-length S peptide mix and cytokine multiplex analysis of supernatants was performed (n=8 per group). Splenocytes of buffer treated mice served as control. Cytokine production was determined by bead-based multiplex analysis (n=8 per group, n=7 for IL-4, IL-5 and IL-13 as one outlier was removed via routs test [Q=1%] for the S peptide stimulated samples). Individual dots indicate results from one animal; group mean values are indicated by bars. P-values were determined by a two-tailed paired t-test.

To dissect the cellular response after BNT162b2 immunization in more detail, mice were immunized with 5 µg BNT162b2 and 12 days after immunization draining lymph nodes (dLNs) were collected to perform B-cell and T-cell phenotyping analysis by flow cytometry (Figure 2.6.2-13). Much higher numbers of B cells (including plasma cells, class switched IgG1- and IgG2a-positive B cells, and germinal center B cells) were observed in the samples from mice that received BNT162b2 compared to controls. In addition, dLNs from BNT162b2-immunized mice also displayed an elevation in T-cell counts, particularly numbers of T follicular helper (Tfh) cells, including subsets with ICOS upregulation, which is known to play an essential role in the formation of germinal centers (Hutloff 2015).

FDA-CBER-2021-5683-0708861

Figure 2.6.2-13.   B- and T-cell Phenotyping in Lymph Nodes of BNT162b2 Immunized Mice
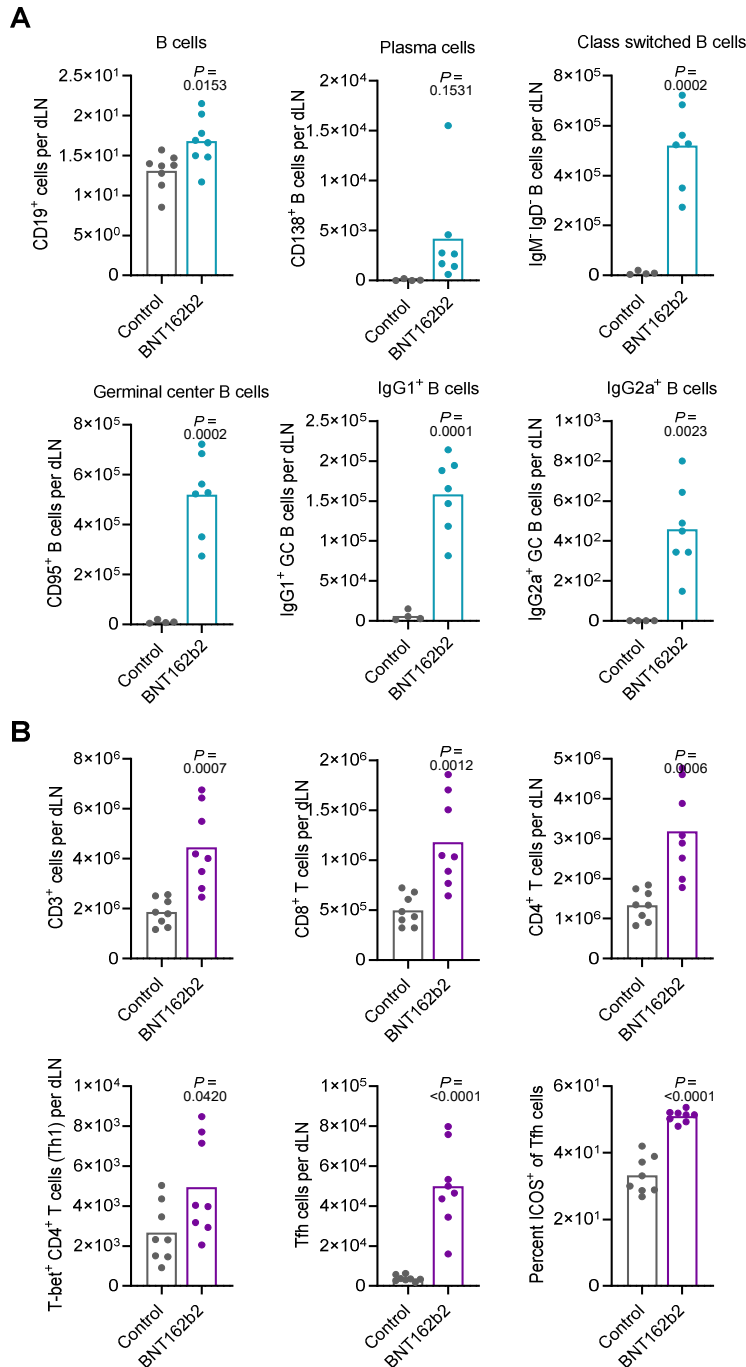
Mice (n=8 per group) were immunized with 5 µg BNT162b2 or buffer (Control). (A) B-cell and (B) T-cell numbers 12 days after immunization in the subsets indicated by the y-axis labels were analysed in draining lymph nodes by flow cytometry. P-values were determined by an unpaired two-tailed t-test. The percentage of ICOS^{+} cells among T follicular helper cells (Tfh) in draining lymph nodes (dLNs) is depicted on the lower right.

FDA-CBER-2021-5683-0708862

In summary, BNT162b2 (V9) induced a strong antibody response, with high total IgG, high binding affinity to S1 and the RBD, and high pVNT titers. Both CD4$^+$ and CD8$^+$ T-cell responses were detectable 12 and 28 days after one immunization with an overall significant increase in T-cell reactivity compared to control animals. Taking the phenotyping of B and T cells in aggregate, the data indicate a strong and concurrent induction of SARS-CoV-2 S-specific neutralizing antibody titers and a Th1-driven T-cell response by BNT162b2.

2.6.2.6. BNT162b2 (V9) Vaccine Immunogenicity and Evaluation of Protection against SARS-CoV-2 Challenge in Rhesus Macaques

The ability of BNT162b2 immunization to protect rhesus macaques from live SARS-CoV-2 challenge was evaluated in 2–4 year old male rhesus macaques (VR-VTR-10671).

2.6.2.6.1. Immunogenicity in Rhesus Macaques

Groups of 2-4 year old male rhesus macaques were immunized IM with 30 or 100 µg of BNT162b2 or saline control on Days 0 and 21. S1-binding IgG was readily detectable after a single immunization, and levels increased further seven days after the second immunization (Day 28) to geometric mean S1-binding IgG concentrations (GMCs) of 30,339 units (U)/mL (30 µg dose level) and 34,668 U/mL (100 µg dose level) (Figure 2.6.2-14). For comparison, the GMC of a panel of 38 SARS-CoV-2 convalescent human sera was 631 U/mL, substantially lower than the GMC of the immunized rhesus macaques after one or two doses.

Human convalescent sera (HCS) were drawn from SARS-CoV-2 infected individuals 18 to 83 years of age, at least 14 days after PCR-confirmed diagnosis, and at a time when individuals were asymptomatic. The serum donors predominantly had symptomatic infections (35/38), and one had been hospitalized. Based on the assumptions that the immune response to SARS-CoV-2 infection provides some measure of protection from disease upon subsequent exposure to the virus and that the neutralizing antibody response contributes to that protection, the neutralizing antibody titer of the convalescent serum panel provides a currently assessable benchmark to judge the quality of the immune response to the vaccine candidates.

Figure 2.6.2-14.   S1-Binding IgG Levels Elicited by Immunization of Rhesus Macaques with BNT162b2
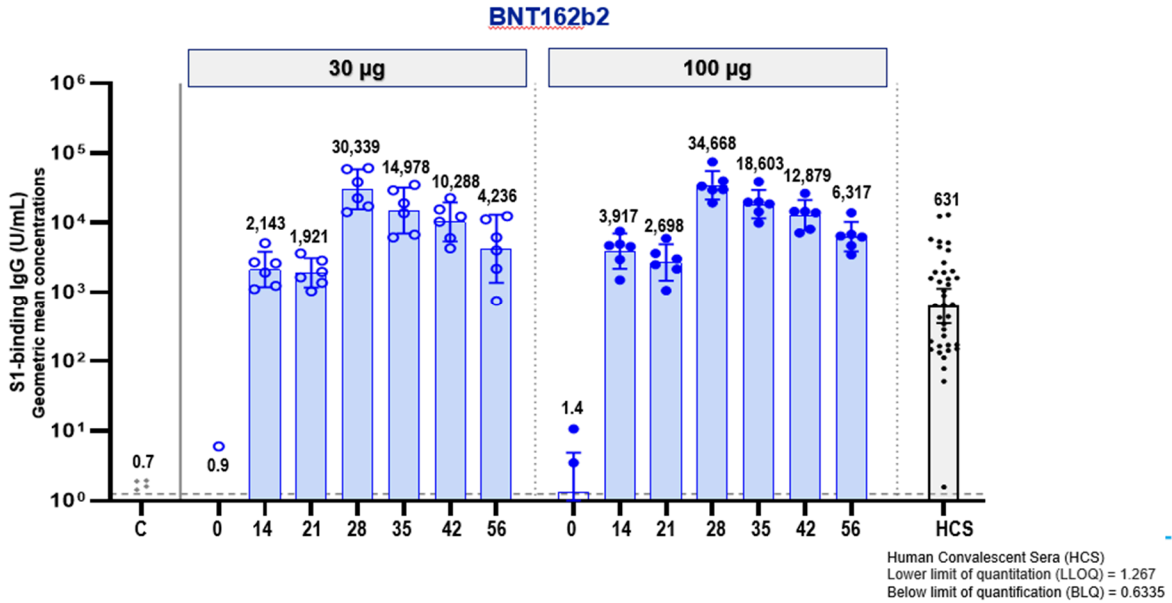
S1-binding IgG concentrations elicited by immunization of rhesus macaques with BNT162b2. Numbers on the x-axis indicate the day post first immunization. Heights of bars indicate geometric mean concentrations (GMCs) in arbitrary units, which are written above the bars; whiskers indicate 95% CIs; dots represent individual monkey IgG concentrations. Dotted line indicates the lower limit of quantification (LLOQ 1.151 U/ml). Values at or below LLOQ were set to ½ LLOQ. C – saline-immunization control; HCS – human convalescent serum panel.

Fifty percent neutralization titers (VNT$_{50}$), measured by an authentic SARS-CoV-2 neutralization assay (Muruato et al, 2020), were detectable in rhesus sera by Day 14 after a single immunization and peaked at geometric mean titers (GMTs) of 962 (on Day 35, 14 days after Dose 2 of 30 µg) or 1,689 (on Day 28, 7 days after Dose 2 of 100 µg; Figure 2.6.2-15). Robust neutralization GMTs of 285 for 30 µg and 310 for 100 µg dose levels persisted to at least Day 56 (most recent time point tested). For comparison, the 50% neutralization GMT of the human convalescent serum panel was 94.

FDA-CBER-2021-5683-0708864

090177e1962f80a2\Approved\Approved On: 04-Feb-2021 00:09 (GMT)

Figure 2.6.2-15.   50% Serum Neutralizing Titers Elicited by Immunization of Rhesus Macaques with BNT162b2
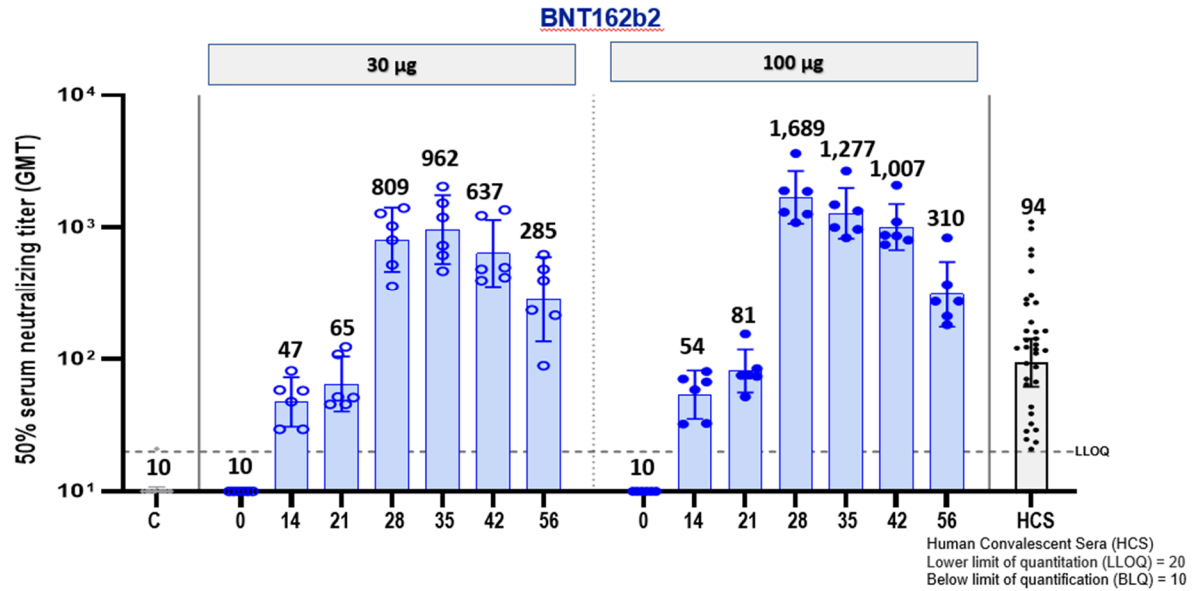
Numbers on the x-axis indicate the day post first immunization. Heights of bars indicate GMTs, which are written above the bars; whiskers indicate 95% confidence intervals; dots represent individual monkey titers. LLOQ – 20. Titers at or below LLOQ were set to ½ LLOQ. C – saline-immunization control; HCS – human convalescent serum panel.

Antigen-specific T-cell responses play an important role in generation of antigen-specific antibody response as well as in elimination of infected cells to mediate protection against disease. S-specific T-cell responses were analyzed in animals immunized with 30 µg or 100 µg of BNT162b2 and unimmunized controls (Control) by ELISpot and intracellular cytokine staining (ICS). PBMCs were collected before immunization (day 0), 14 days post dose 1 (14d PD1), 7 days post dose 2 (7d PD2), and 21 days post Dose 2 (21d PD2).

S-specific T cells were low to undetectable in naïve animals. Strong IFNγ ELISpot responses but minimal IL-4 ELISpot responses were detected after the second 30 or 100 µg dose of the vaccine candidate (Figure 2.6.2-16). ICS confirmed that BNT162b2 elicited strong S-specific IFNγ producing T cell responses, including a high frequency of CD4+ T cells that produced IFNγ, IL-2, or TNF-α but a low frequency of CD4+ cells that produce IL-4, indicating a Th1-biased response (Figure 2.6.2-17A through D). BNT162b2 also elicited S-specific IFNγ producing CD8+ T cell responses (Figure 2.6.2-17E).

FDA-CBER-2021-5683-0708865

Figure 2.6.2-16.   IFNγ and IL-4 ELISpot Results in BNT162b2 Immunized Animals
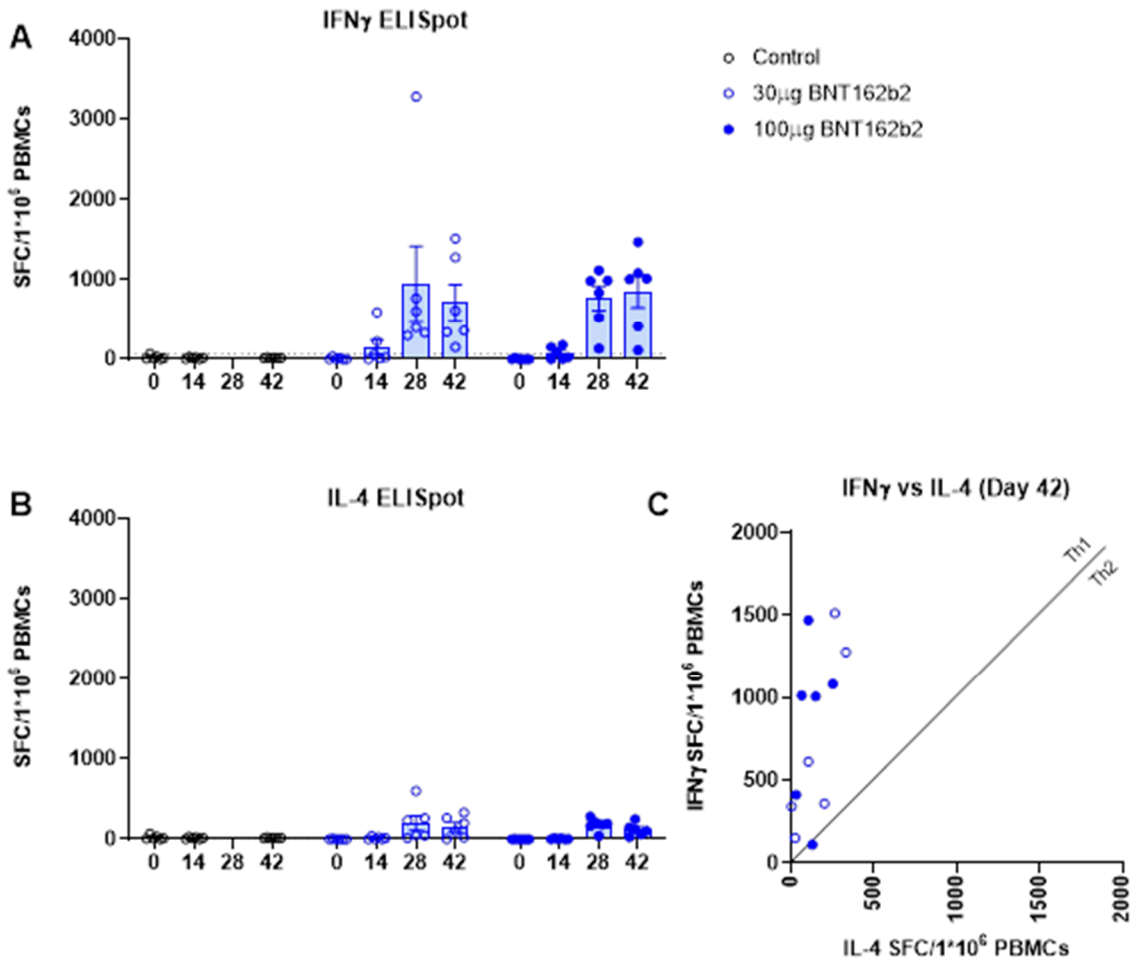
Groups of six 2-4 year old rhesus macaques were immunized on Days 0 and 21 with 30 or 100 μg BNT162b2 or buffer (Placebo). Height of bars indicates the mean; whiskers indicate the standard error of mean (SEM); and each symbol represents one animal. Dotted lines mark the lower limit of detection. (A) IFNγ (B) IL-4 ELISpot analysis. (C) Correlation of frequency of IFNγ or IL-4 producing cells 21 days PD2.

FDA-CBER-2021-5683-0708866

Figure 2.6.2-17. S-specific CD4 and CD8 T-cell Response in BNT162b2 Immunized Animals as Measured by ICS Assay
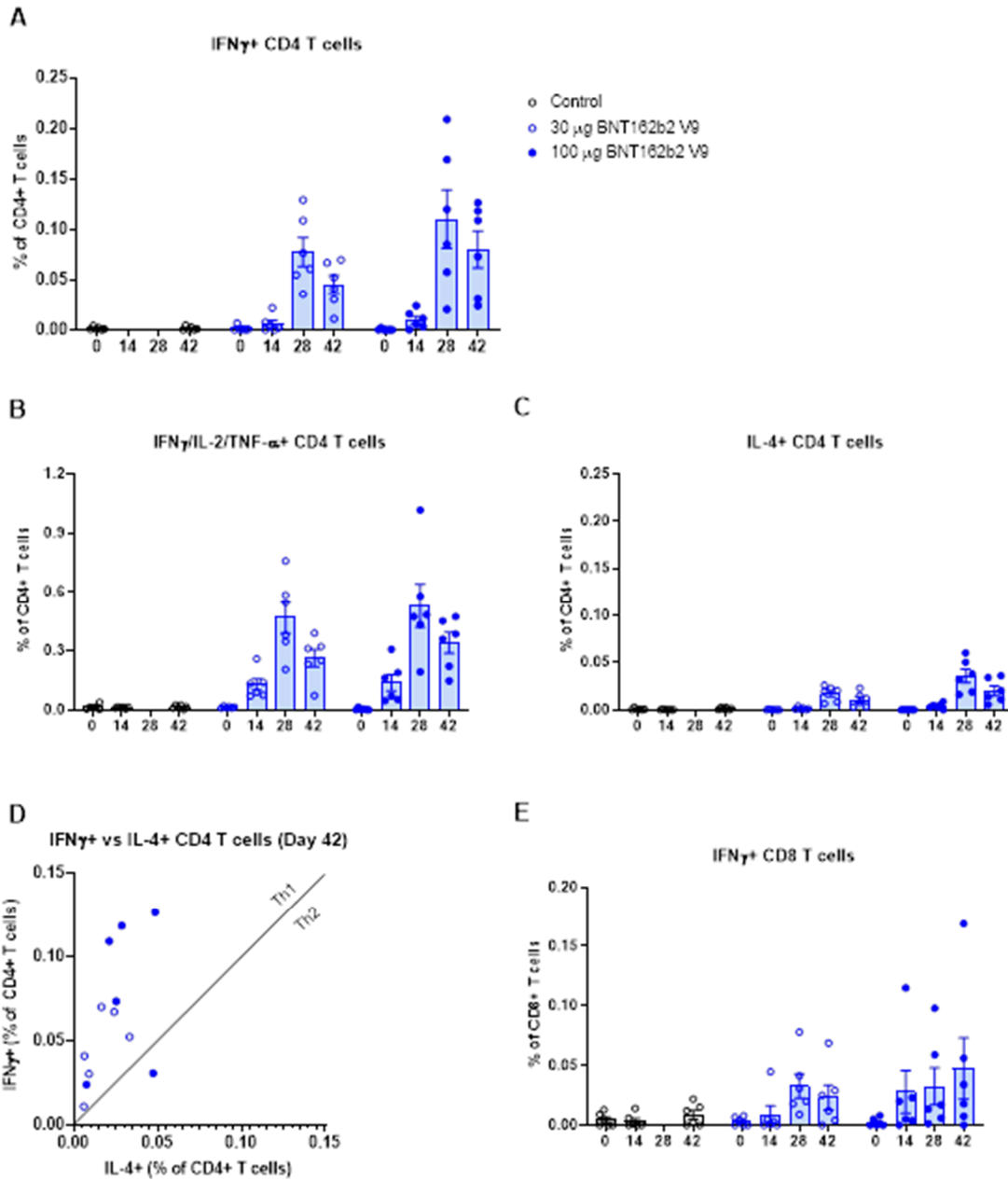
Height of bars indicates the mean; whiskers indicate the standard error of mean (SEM); and each symbol represents one animal. (A) Frequency of IFNγ[+] CD4 T cells. (B) Frequency of IFNγ/IL-2/TNF-α[+] CD4 T cells (C) Frequency of IL-4^{+} CD4 T cells. (D) Correlation of frequency of IFNγ or IL-4^{+} CD4 T cells at 21 days PD2. (E) Frequency of IFNγ[+] CD8 T cells.

FDA-CBER-2021-5683-0708867

2.6.2.6.2. SARS-CoV-2 Challenge of BNT162b2 (V9)-Immunized Nonhuman Primates

SARS-CoV-2 infection and COVID-19 in humans present diverse manifestation of signs, symptoms, and severity. Based on published reports, SARS-CoV-2 challenged rhesus macaques develop an acute, transient infection in the upper and lower respiratory tract and have evidence of viral replication in the gastrointestinal tract, similar to humans (Zou et al, 2020; Kim et al, 2020). Varying degrees of pulmonary inflammation, primarily at the peak of infection at approximately day 2 to 4 post-challenge, have been reported in the literature (Munster et al, 2020). The human and rhesus ACE2 receptor have 100% amino acid identity at the critical binding residues, which may account for the fidelity of this SARS-CoV-2 animal model (Zhou et al, 2020).

The groups of 2-4 year old male rhesus macaques that had received two intramuscular immunizations with 100 µg BNT162b2 (V9) (n=6) or buffer (Control; n=3) 21 days apart (described in Section 2.6.2.6.1) were challenged 55 days after the second immunization with 1.05×10^6 plaque forming units of SARS-CoV-2 (strain USA-WA1/2020), split equally between the intranasal and intratracheal routes, as previously described (Singh et al, 2020). Three additional non-immunized, age-matched, rhesus macaques (sentinel) were mock-challenged with cell culture medium. Nasal and oropharyngeal (OP) swabs were collected and bronchoalveolar lavage (BAL) was performed at the times indicated, and the samples were tested for the presence of SARS-CoV-2 RNA (genomic RNA and subgenomic transcripts) by reverse-transcription quantitative polymerase chain reaction (RT-qPCR; Figure 2.6.2-18). All personnel performing the clinical, radiographic, histopathologic, and RT-qPCR evaluations were blinded to the group assignments of the macaques (VR-VTR-10671).

All samples obtained before the infectious challenge and all those obtained from sentinel animals lacked detectable SARS-CoV-2 RNA (Figure 2.6.2-18). Viral RNA was detected in BAL fluid from 2 of the 3 control-immunized macaques on Day 3 after challenge and from 1 of 3 on Day 6. At no time point sampled was viral RNA detected in BAL fluid from the BNT162b2 (V9)-immunized and SARS-CoV-2 challenged macaques (Figure 2.6.2-18A). The difference in viral RNA detection in BAL fluid between BNT162b2-immunized and control-immunized rhesus macaques after challenge is statistically significant (p=0.0014).

From control-immunized macaques, viral RNA was detected in nasal swabs obtained on Days 1, 3, and 6 after SARS-CoV-2 challenge; from BNT162b2 (V9)-immunized macaques, viral RNA was detected only in nasal swabs obtained on Day 1 after challenge and not in swabs obtained on Day 3 or subsequently (Figure 2.6.2-18B). The pattern of viral RNA detection from OP swabs was similar to that for nasal swabs (Figure 2.6.2-18C).

**Figure 2.6.2-18.   Viral RNA in BAL Fluid and Nasal and Oropharyngeal Swabs of
Rhesus Macaques after Infectious SARS-CoV-2 Challenge**

FDA-CBER-2021-5683-0708869
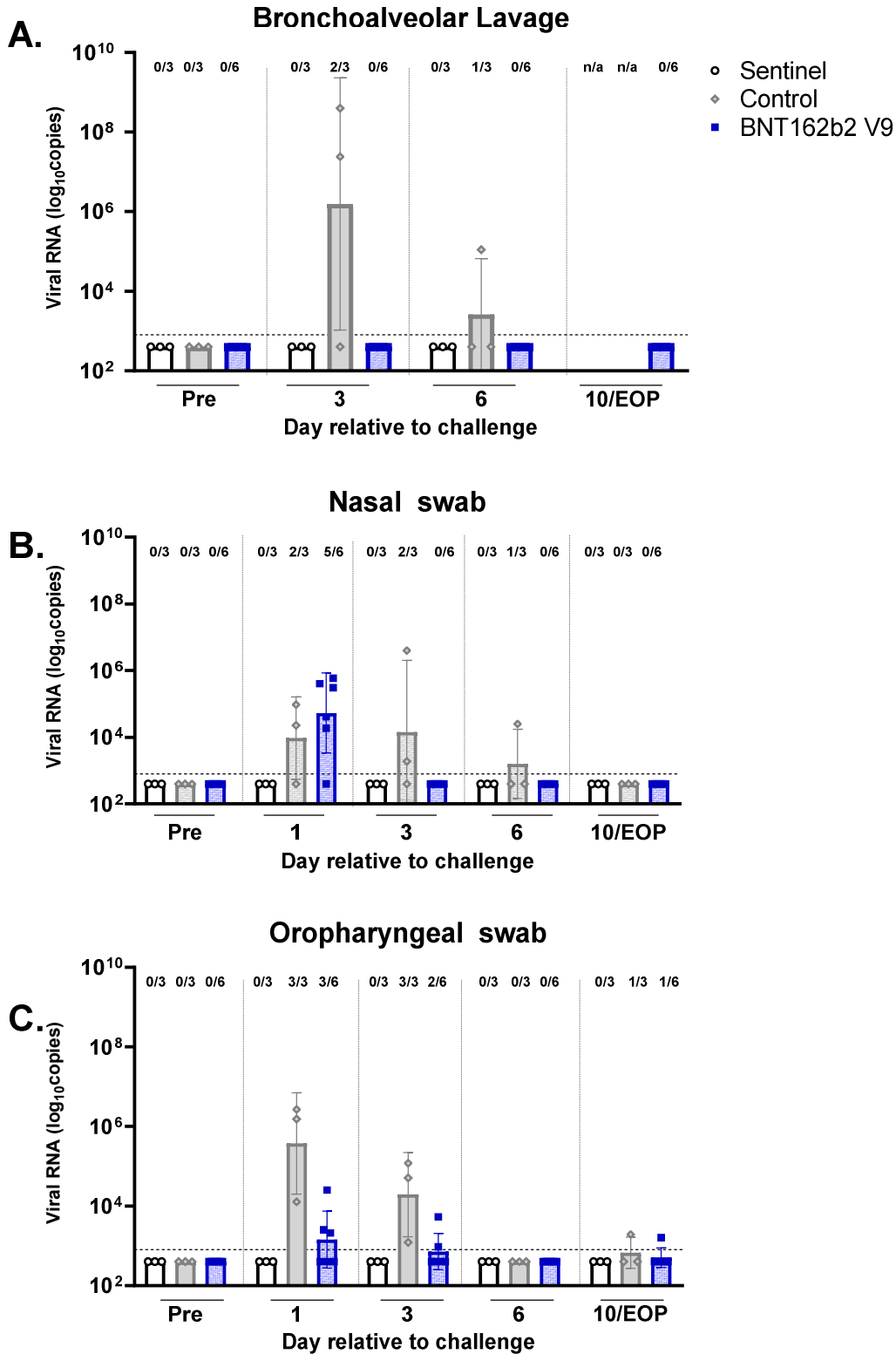
090177e1962f80a2\Approved\Approved On: 04-Feb-2021 00:09 (GMT)

Groups of 2-4 year old rhesus macaques were immunized on days 0 and 21 with 100 µg BNT162b2 (V9) (n=6), or buffer (Control; n=3). Fifty-five days after the second immunization, the animals were challenged with 1.05×10^6 pfu of SARS-CoV-2 split equally between the IN and IT routes. Three age-matched male rhesus macaques were unimmunized and challenged with cell culture medium only (Sentinel). Viral RNA levels were detected by RT-qPCR in A) bronchoalveolar lavage, B) nasal swabs, and C) oropharyngeal swabs. EOP, end of project. Values below the LLOD set to ½ the LLOD. The viral RNA levels between control-immunized and BNT162b2-immunized animals after challenge were compared by a non-parametric analysis (Friedman's test), and the p-values are 0.0014 for BAL fluid, 0.2622 for nasal swabs, and 0.0007 for OP swabs. The Friedman's test is a non-parametric analysis based on the ranking of viral RNA shedding data within each day. PROC RANK and PROC GLM from SAS® 9.4 were used to calculate the p-values.

Despite the presence of viral RNA in BAL fluid from challenged control animals, none of the challenged animals, immunized or control, showed clinical signs of illness (Figure 2.6.2-19), indicating that the 2-4 year old male rhesus monkey challenge model appears to be an infection model, but not a clinical disease model. Lung radiograph (Figure 2.6.2-20A) and computerized tomography (CT) (Figure 2.6.2-20B) scores were determined by two board-certified veterinary radiologist who were blinded to treatment group. Data in Figure 2.6.2-20 represent the average of the two scores. Radiographic evidence of pulmonary abnormality was observed in challenged controls but not in challenged BNT162b2-immunized animals nor in unchallenged sentinels. No radiographic evidence of vaccine-elicited enhanced disease was observed. At necropsy on Day 7 or 8 after virus challenge, there were no significant gross pathology findings in any organs. Microscopically, the main finding in the lung was inflammation. The lung inflammation area score was similar between saline-immunized and BNT162b2-immunized animals, and there was no evidence of enhanced respiratory disease (Figure 2.6.2-21).

Overall, these data demonstrate that, compared to control, BNT162b2 (V9) immunization provided complete protection in the lungs from infectious SARS-CoV-2 challenge in rhesus macaques with no evidence of vaccine-elicited disease enhancement.

Figure 2.6.2-19.   Clinical Signs in Rhesus Macaques after Immunization with BNT162b2 and Challenge with Infectious SARS-CoV-2
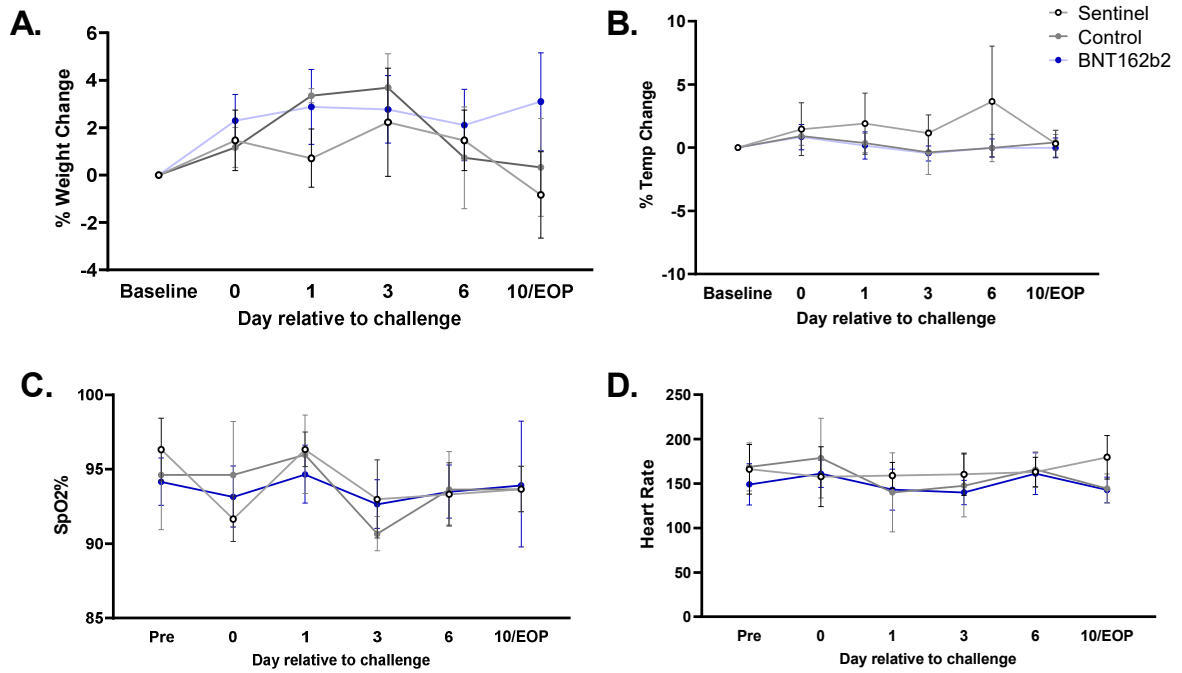
Rhesus macaques were immunized with BNT162b2 (V9), or saline, and challenged with SARS-CoV-2 or cell culture medium as described in the Figure 2.6.2-18 legend. Clinical signs were recorded on the days indicated. EOP, end of project. BNT162b2-immunized (n=6), control (n=3), and sentinel (n=3) macaques. A, Body weight. B, Temperature. C, Oxygen saturation. D, Heart rate.

FDA-CBER-2021-5683-0708871

Figure 2.6.2-20.   Radiograph and CT Scores of Rhesus Macaque Lungs after Infectious SARS-CoV-2 Challenge
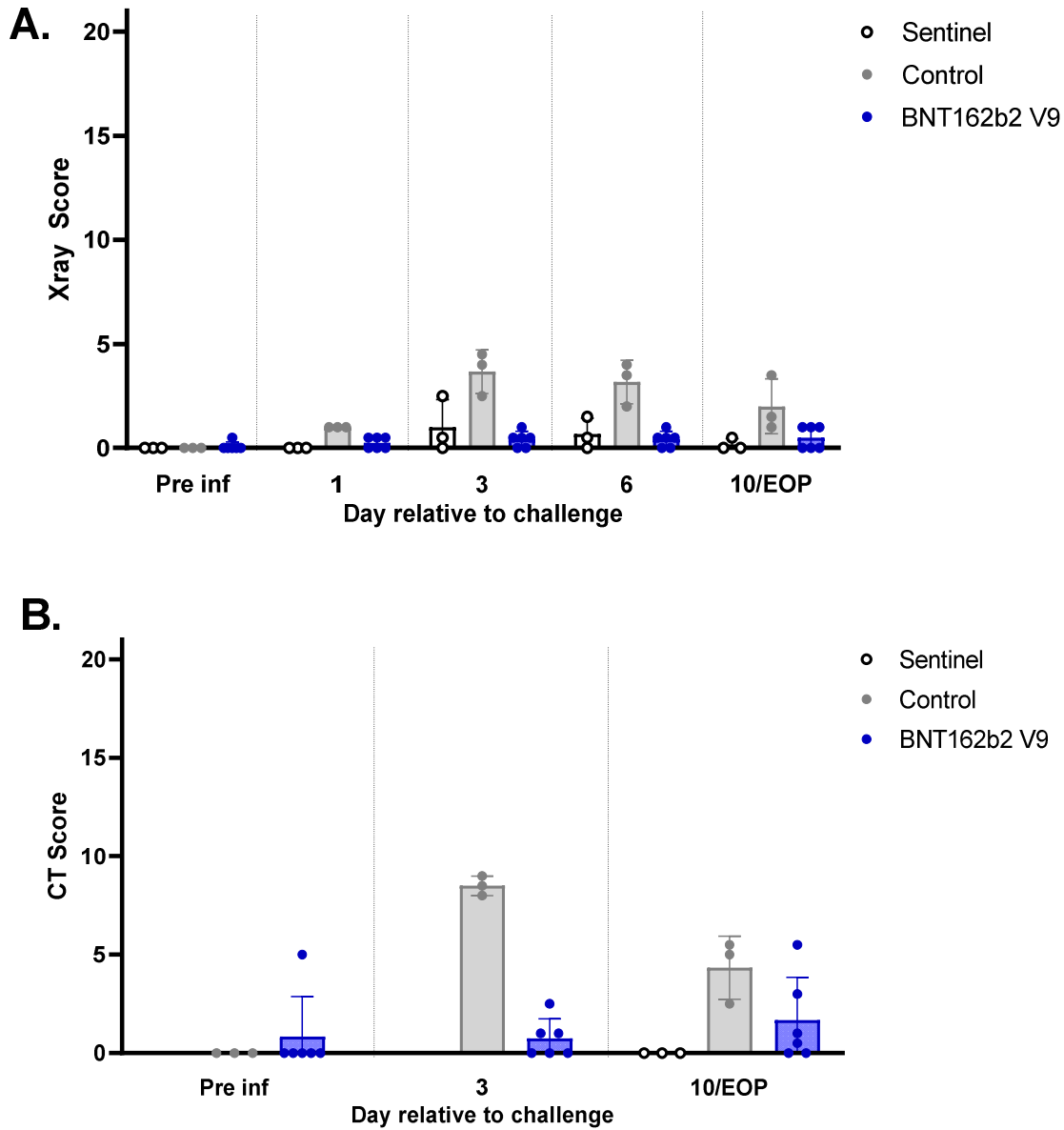
Fifty-five days after the second immunization, BNT162b2 or Control (saline)-immunized animals were challenged with 1.05×10^6 pfu of SARS-CoV-2 split equally between the IN and IT routes. Three age-matched unimmunized rhesus macaques were challenged with cell culture medium only (Sentinel). Chest X-rays and CT scans were performed prior to challenge and at the times indicated on the x-axis. EOP, end of project. Radiograph (A) and CT (B) scores were assigned to a total of 7 regions on a scale of 1-20. Images were evaluated by two board-certified veterinary radiologists blinded to treatment group. Individual data points represent the average of the two scores. The height of the bars indicates the mean score. Error bars indicate the standard deviation.

FDA-CBER-2021-5683-0708872

Figure 2.6.2-21.   Lung Inflammation Area Score after IN/IT SARS-CoV-2 Challenge
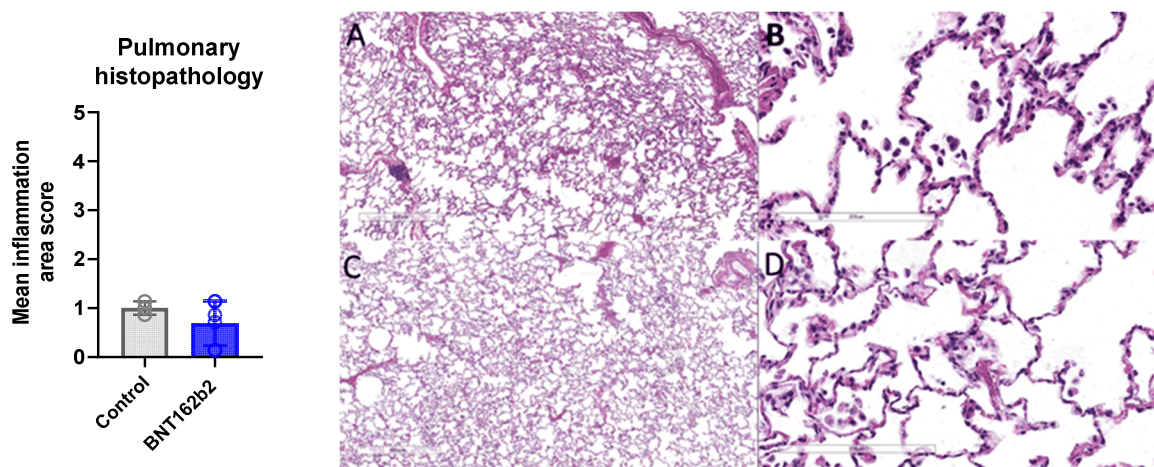
Graph (left panel): Lung inflammation area score on Day 7 or 8 after IN/IT SARS-CoV-2 challenge. Each data point represents the mean lung inflammation area score of a single animal (mean score of the 7 lung lobes). Saline-immunized and challenged animals (Control; n=3) are shown in grey and BNT162b2-vaccinated and challenged animals (BNT162b2; n=6) are shown in blue. Each dot represents the inflammation mean area score for an individual animal. Bars indicate the geometric mean area scores within each group. Photomicrographs (right panel; 2.5x objective, A and C; 20x objective, B and D) of hematoxylin and eosin-stained lung sections from Control animals (A and B) and lungs from BNT162b2-immunized and challenged animals (C and D).

2.6.2.7. Immunogenicity Testing of Rats in the GLP Compliant Repeat Dose Toxicity Studies and Developmental and Reproductive Toxicity Study

Immunogenicity results from two GLP-compliant repeat-dose toxicity studies, one (Study 20GR142) with BNT162b2 (V9) and one (Study 38166) with its closely related variant BNT162b2 (V8), as well as a DART study (Study 20256434) with BNT162b2 (V9) are presented below.

2.6.2.7.1. Repeat-Dose Toxicity Study of Three LNP-Formulated RNA Platforms Encoding for Viral Proteins by Repeated Intramuscular Administration to Wistar Han Rats

The immunogenicity of BNT162b2 (V8) in the GLP--compliant repeat-dose rat toxicity study (Study 38166) was analyzed. BNT162b2 (V8) has an alternative coding sequence to the Phase 2/3 study clinical candidate and subject of this application, BNT162b2 (V9), with V9 containing a higher content of cytosine ribonucleotides for increased protein expression. Both variants, V8 and V9, encode the identical protein, and in this toxicology study, the V8 was a surrogate for BNT162b2 (V9).

Male and female Wistar Han rats received three weekly doses of 100 µg of BNT162b2 (V8). Serum samples were collected and analyzed (5 animals/sex) from main study animals on Day 17, two days after the 3rd administration, at the end of the dosing phase as well as from recovery cohorts at the end of the study on Day 38. Treatment with the BNT162b2 vaccine elicited binding IgG against the S1 fragment and the RBD of SARS-CoV2 S. There was a

FDA-CBER-2021-5683-0708873

strong antibody response at both analyzed time points. The group mean IgG concentration against S1 and RBD are given in Table 2.6.2-2. Antibody concentrations against S1 and RBD increased over time.

Table 2.6.2-2. IgG antibody Concentration [mg/mL] Against the Viral Antigen in Wistar Han Rats after BNT162b2 (V8) Immunization

		BNT162b2 (100 μg)
17 days after first immunization	**Against S1**	1.76 ± 0.16
	Against RBD	2.33 ± 0.19
38 days after first immunization	**Against S1**	3.46 ± 0.52
	Against RBD	4.90 ± 0.87

Pseudovirus neutralization results mirrored the antigen binding results.

Treatment of rats with BNT162b2 (V8) resulted in the elicitation of neutralizing antibodies against pseudovirus infection. Neutralizing antibody titers in vaccinated animals increased over time with the recorded neutralizing activity being consistent with the ELISA data shown above. Serum titers resulting in 50% pseudovirus neutralization exceeded the upper limit of quantification (ULOQ) of a reciprocal titer of 1536 in more than 8 out of 10 animals on Day 38, and therefore a neutralization titer of 90% was evaluated as well (Figure 2.6.2-22).

Figure 2.6.2-22.   Pseudovirus Neutralization Activity in Rats after BNT162b2 V8 Immunization
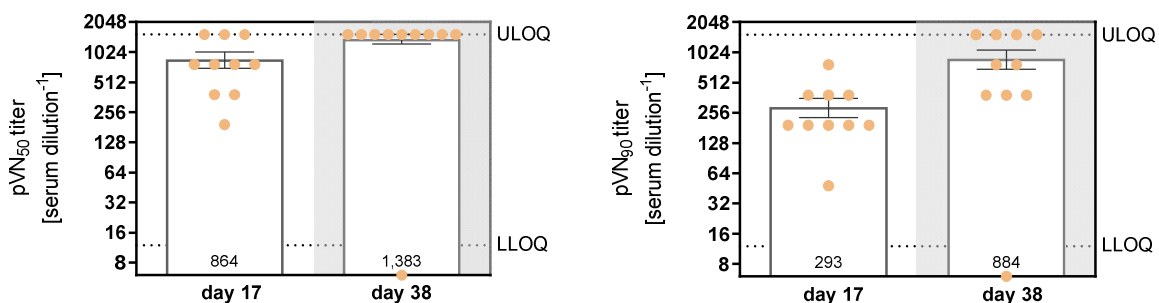
Wistar Han rats were immunized IM with three weekly injections of 100 μg BNT162b2. On Day 17 and Day 38, animals were bled, and the sera were tested for titers of pseudovirus neutralizing antibodies. Individual titers resulting in 50% pseudovirus neutralization ($pVNT_{50}$, left graph) or 90% pseudovirus neutralization ($pVNT_{90}$, right graph) are shown by dots; group mean values are indicated by horizontal bars and are included in the figure ($\pm$SEM, standard error of the mean). Group size for analysis was n=5 male and n=5 female rats. Mean titers are given in the bars. All control serum samples were below the lower limit of quantification (LLOQ); ULOQ = upper limit of quantification.

FDA-CBER-2021-5683-0708874

2.6.2.7.2. 17-Day Intramuscular Toxicity Study of BNT162b2 (V9) in Wistar Han Rats With a 3-Week Recovery

The immunogenicity of the COVID-19 vaccine candidate BNT162b2 (V9) (and BNT162b3c) in the GLP compliant repeat-dose rat toxicity study (Study 20GR142) was analyzed. The summary of the results described below will focus on only the BNT162b2 (V9) candidate.

Wistar Han rats (15/sex/group) were administered IM doses of 0 (saline) or 30 BNT162b2 (V9) µg RNA/dose per animal. Doses were administered once a week for 3 weeks (Days 1, 8, and 15). Following the dosing phase, 10 animals/sex from each group were euthanized 2 days post last immunization for post-mortem assessments. The remaining 5 animals/sex/group were euthanized following a 3-week recovery phase.

Administration of 3 once-weekly doses of BNT162b2 (V9) elicited SARS-CoV-2 neutralizing antibody responses in males and females at the end of the dosing (Day 17) and recovery (Day 21) phases of the study. SARS-CoV-2 neutralizing antibody responses were not observed in animals prior to vaccine administration or in saline-administered control animals (Table 2.6.2-3).

Table 2.6.2-3. Group Mean Titers of SARS-CoV-2 Neutralizing Antibodies

Study Day	Sex	Saline (0 µg RNA)	BNT162b2 (V9) (30 µg RNA)
Prior to Dosing Initiation (Day -5)	Male	5	5
	Female	5	5
End of Dosing Phase (Day 17)	Male	5	1114
	Female	5	2501
End of Recovery Phase (RP Day 21)	Male	5	5120
	Female	5	5120

RP = Recovery phase.

2.6.2.7.3. A Combined Fertility and Developmental Study (Including Teratogenicity and Postnatal Investigations) of BNT162b1, BNT162b2 and BNT162b3 by Intramuscular Administration in the Wistar Han Rat

The immunogenicity of the COVID-19 vaccine candidate BNT162b2 (V9) (and BNT162b3c) in the GLP compliant DART (Study 20256434) was analyzed. The summary of the results described below will focus on only the BNT162b2 (V9) candidate.

Female Wistar Han rats (44 animals/group) were administered saline or 30 µg RNA/dosing day of BNT162b2 (V9) by IM injection for a total of 4 doses (21 and 14 days prior to mating and on GDs 9 and 20). On GD 21, half of the females in each group underwent Caesarean section. The remaining females in each group were allowed to naturally deliver their pups and both maternal animals and their offspring were monitored out through the end of weaning (LD 21/PND 21). SARS-CoV-2 neutralizing antibodies were assessed in maternal animals prior to mating, on GD 21, and LD 21 as well as in fetuses on GD 21 and in pups on PND 21.

FDA-CBER-2021-5683-0708875

BNT162b2 elicited SARS-CoV-2 neutralizing antibody responses in all of the females just prior to mating (M 0), at the end of gestation (GD 21), and at the end of lactation (LD 21). SARS-CoV-2 neutralizing titers were detected in all offspring (fetuses on GD 21 and pups on PND 21). SARS-CoV-2 neutralizing antibody titers were not observed in animals prior to vaccine administration or in saline-administered control animals (Table 2.6.2-4).

Table 2.6.2-4. Group Mean Titers of SARS-CoV-2 Neutralizing Antibodies

Interval/Occasion	Saline (0 μg RNA)	BNT162b2 (V9) (30 μg RNA)
Prior to Dosing Initiation	5.0	5.3
Just Prior to Mating	5.0	3886.4
Gestation Day 21 (Dams)	5.0	3445.5
Lactation Day 21	5.0	3620.4
Fetuses (Gestation Day 21)	5.0	640.0
Pups (Postnatal Day 21)	5.0	4561.4

2.6.2.8. Secondary Pharmacodynamics

No secondary pharmacodynamics studies were conducted with BNT162b2.

2.6.2.9. Safety Pharmacology

No safety pharmacology studies were conducted with BNT162b2 as they are not considered necessary according to the WHO guideline (WHO, 2005).

2.6.2.10. Pharmacodynamic Drug Interactions

Pharmacodynamic drug interaction studies with BNT162b2 have not been conducted.

2.6.2.11. Discussion and Conclusions

The BNT162b2 vaccine candidate encoding the full-length P2 S induces robust immune responses in mice, rats, and nonhuman primates. SARS-CoV-2 S is a primary target of neutralizing antibodies, and the modRNA that encodes the vaccine antigen induces a strong neutralizing antibody response, Th1-type $CD4^+$ T-cell response, and a $CD8^+$ IFNγ response. This diversity of elicited immune mechanisms could block virus infection as a first line of defense and clear virus-infected cells as a second line of defense.

A recombinant form of the P2 S antigen encoded by the vaccine and transiently expressed on the surface of mammalian cells was bound by a soluble ACE2 receptor and SARS-CoV-2 neutralizing monoclonal antibodies with high affinities. Analysis of the P2 S trimer structure by cryoelectron microscopy revealed high similarity to previously reported P2 S structures. The well-resolved trimeric prefusion structure and the high affinity binding to ACE2 and human neutralizing antibodies demonstrate that the recombinant full-length P2 S authentically presents the ACE2 binding site and other epitopes targeted by many SARS-CoV-2 neutralizing antibodies.

Nonclinical studies in mice and nonhuman primates showed that antigen-binding IgG and neutralizing antibody responses were detectable as early as 14 d post-immunization, with

FDA-CBER-2021-5683-0708876

substantial increases observed in nonhuman primates after the second dose. Similar results indicating immunogenicity were obtained in an accessory study to the GLP-compliant repeat-dose toxicology studies in rats (Study 38166 and Study 20GR142) and DART study (Study 20256434). In a SARS-CoV-2 rhesus challenge model, BNT162b2 provided partial protection from infection in the upper airway, and no viral RNA was detected in the lower airways, sampled serially by BAL starting 3 days after challenge. No evidence of disease enhancement was observed in BNT162b2-immunized and SARS-CoV-2 challenged macaques (VR-VTR-10671).

2.6.2.12. Immunogenicity and Efficacy Methods

2.6.2.12.1. SARS-CoV-2 S1 and RBD Direct ELISA

For preclinical studies in mice, antigen-based direct ELISAs measured S1-binding (S1 recombinant protein, Sino Biological) and RBD-binding (recombinant RBD, Sino Biological) IgG levels in serum samples. MaxiSorp plates (Thermo Fisher Scientific) were coated with recombinant protein (100 ng/100 µL) in sodium carbonate buffer, and bound IgG was detected using an HRP-conjugated secondary antibody and TMB substrate (Biotrend). Data collection was performed using a BioTek Epoch reader and Gen5 software version 3.0.9. For concentration analysis, the signal of the specific samples was correlated to a standard curve of an isotype control.

2.6.2.12.2. VSV/SARS-CoV-2 S Pseudovirus Neutralization Assay

For preclinical immunogenicity studies in rodents, a pseudotype neutralization assay (pVNT) was used as a surrogate of virus neutralization (which, for SARS-CoV-2, requires BSL3 containment). The pVNT is based on a recombinant replication-deficient vesicular stomatitis virus (VSV) vector that encodes GFP instead of VSV-G (VSVΔG-GFP). VSVΔG-GFP was pseudotyped with SARS-CoV-2 S protein according to published pseudotyping protocols (Berger & Zimmer 2011; Baum et al, 2020). Serial dilutions of mouse sera were incubated with the pseudotyped reporter virus for 10 minutes at room temperature before inoculating Vero-76 cell monolayers in 96 well plates. Virus was added at 300 IU per well and infected cell counts per well were detected 16-24 hours after inoculation with an IncuCyte Live Cell Analysis system (Sartorius) with IncuCyte 2019B Rev2 software. The 50% pseudovirus neutralization titer ($pVNT_{50}$) was reported as the reciprocal of the first serum dilution yielding a 50% reduction in GFP-positive infected cell number per well compared to the mean of the no serum pseudovirus positive control.

2.6.2.12.3. SARS-CoV-2 S1-Binding and RBD-Binding Kinetics using Surface Plasmon Resonance Spectroscopy

Binding kinetics of murine S1- and RBD-binding serum IgGs was determined using a Biacore T200 device (Cytiva). An anti-mouse-Fc antibody (Jackson ImmunoResearch) was covalently coupled to immobilization level of ~10,000 response units (RU) on the CM5 sensor chip matrix. Bulk mouse IgGs were captured from diluted serum and binding analyses to histidine-tagged S1 (S1-His) or histidine-tagged RBD (RBD-His) (Sino Biological) were performed using a multi-cycle kinetic method with concentrations ranging from 25 to 400 nM or 1.5625 to 50 nM, respectively. Binding kinetics were calculated using a global

FDA-CBER-2021-5683-0708877

kinetic fit to a 1:1 Langmuir model with Biacore T200 Evaluation Software Version 3.1 (Cytiva).

2.6.2.12.4. SARS-CoV-2 S1-Binding IgG Luminex Assay

For nonhuman primate studies, a direct binding Luminex immunoassay (dLIA) was used to quantify S1-binding serum IgG levels (VR-MQR-10211). A recombinant SARS-CoV-2 S1 with a C-terminal Avitag™ (Acro Biosystems) was bound to streptavidin-coated Luminex microspheres. Bound nonhuman primate S1-binding IgG was detected with a R-Phycoerythrin-conjugated goat anti-human polyclonal secondary antibody (Jackson Labs). Data were captured as median fluorescent intensities (MFIs) using a Luminex reader and converted to U/mL antibody concentrations using a reference standard curve with arbitrary assigned concentrations of 100 U/mL and accounting for the serum dilution factor. Assay results were reported in U/mL of IgG.

2.6.2.12.5. SARS-CoV-2 Neutralization Assay

For nonhuman primate studies, the same authentic SARS-CoV-2 neutralization assay used for clinical testing was applied (VR-MQR-10214). The SARS-CoV-2 neutralization assay used a previously described strain of SARS-CoV-2 (USA_WA1/2020) that had been rescued by reverse genetics and engineered by the insertion of an mNeonGreen (mNG) gene into open reading frame 7 of the viral genome (Xie et al, 2020). This reporter virus generates similar plaque morphologies and indistinguishable growth curves from wild-type virus (Muruato et al, 2020). Viral master stocks used for the neutralization assay were grown in Vero E6 cells as previously described (Xie et al, 2020). Serial dilutions of heat inactivated sera were incubated with the reporter virus for 1 hour at 37 °C before inoculating Vero CCL81 cell monolayers in 96 well plates to allow accurate quantification of infected cells. Virus was added at 2×10^4 PFU per well to yield a target of 10-30% of infected cells in the monolayer. Total cell counts per well were enumerated by nuclear stain (Hoechst 33342) and fluorescent virally infected foci were detected 16-24 hours after inoculation with a Cytation 7 Cell Imaging Multi-Mode Reader (Biotek) with Gen5 Image Prime version 3.09. Titers were calculated in GraphPad Prism version 8.4.2 by generating a 4-parameter (4PL) logistical fit of the percent neutralization at each serial serum dilution. The 50% neutralization titer was reported as the interpolated reciprocal of the dilution yielding a 50% reduction in fluorescent viral foci.

2.6.2.12.6. ELISpot and Cytokine Profiling Immunoassays in Mice

Spleen single-cell suspensions were prepared in PBS by mashing tissue against the surface of a 70 μm cell strainer (BD Falcon). Erythrocytes were removed by hypotonic lysis. Popliteal, inguinal and iliac lymph nodes were pooled, cut into pieces, digested with collagenase D (1 mg/mL; Roche) and passed through cell strainers.

ELISpot assays were performed with mouse IFNγ ELISpot[PLUS] kits according to the manufacturer's instructions (Mabtech). A total of 5×10^5 splenocytes was *ex vivo* restimulated with the full-length S peptide mix (0.1 µg/mL final concentration per peptide, JPT) or controls (gp70-AH1 [SPSYVYHQF] (Slansky et al, 2000), JPT). Streptavidin-ALP and BCIP/NBT-plus substrate were added, and spots counted using an ELISpot plate reader (ImmunoSpot® S6 Core Analyzer, CTL). Spot numbers were evaluated using

FDA-CBER-2021-5683-0708878

ImmunoCapture Image Aquision Software V7.0 and ImmunoSpot 7.0.17.0 Professional. For T-cell subtyping, CD8^{+} T cells were isolated from splenocyte suspensions using MACS MicroBeads (CD8a [Ly-2], Miltenyi Biotec) according to the manufacturer's instructions. The flow-through served as a source of CD4^{+} T cells. CD8^{+} or CD4^{+} T cells were subsequently restimulated with syngeneic bone marrow-derived dendritic cells loaded with full-length S peptide mix (0.1 µg/mL final concentration per peptide) or medium as control.

For cytokine profiling in mice by bead-based immunoassays, mouse splenocytes were re-stimulated for 48 h with full-length S peptide mix (0.1 µg/mL final concentration per peptide) or cell culture medium (no peptide) as control. Concentrations of IFNγ, IL-2, IL-4, IL-5 and (for splenocytes from BNT162b2-immunised mice) IL-13 in supernatants were determined using a bead-based, 11-plex TH1/TH2 mouse ProcartaPlex multiplex immunoassay (Thermo Fisher Scientific) according to the manufacturer's instructions. Fluorescence was measured with a Bioplex200 system (Bio-Rad) and analysed with ProcartaPlex Analyst 1.0 software (Thermo Fisher Scientific). Values below the lower limit of quantification (LLOQ) were set to zero.

2.6.2.12.7. ELISpot and Intracellular Cytokine Staining Assays in NHPs

Cryopreserved NHP PBMCs were thawed in pre-warmed AIM-V media (Thermo Fisher Scientific, US) with Benzonase (EMD Millipore, US), washed once, and the concentration was adjusted to 2.5 x 10^6 cells/mL in AIM-V.

For ELISpot assays, commercially available NHP IFNγ and IL-4 ELISpot assay kits were used (Mabtech, Sweden). Briefly, pre-coated PVDF 96-well microplates were washed with PBS and blocked with AIM-V. PBMCs were added at 1.0 x 10^5 cells/well for IFNγ and 2.5 x 10^5 cells/well for IL-4. Cells were stimulated with a peptide pool spanning the entire S protein (15 mers, 11aa overlap, JPT, Germany) at 1 µg/mL for 24 hours for IFNγ and 48 hours for IL-4 at 37 °C in 5% CO$_2$. Tests were performed in triplicate wells; media-DMSO, a CMV peptide pool (JPT, Germany) and PHA (Sigma, USA) were included as controls. Cells were removed, plates washed, and spots detected using a biotinylated detection antibody followed by a Streptavidin-HRP secondary antibody and AEC chromogenic substrate (BD, US) for 10 minutes for IFNγ and 30 minutes for IL-4 at room temperature until red spots were developed. Dried plates were scanned and counted using a CTL ImmunoSpot S6 Universal Analyzer (CTL, US). Reported results are background (media-DMSO) subtracted and normalized to spot forming cells (SFC)/10^6 PBMCs.

For intracellular cytokine staining (ICS) flow cytometry-based analysis, thawed PBMCs rested for 3 to 4 hours were stimulated in AIM-V medium in 96-well plates with the peptide pool spanning the entire S protein at 1 µg/mL; Staphylococcus enterotoxin B (SEB; 2 µg/mL) was used as a positive control; and 0.2 % DMSO was used as a negative control. An APC-conjugated CD107a monoclonal antibody, GolgiStop, and GolgiPlug were added to each well, and cells were incubated at 37 °C for 12 to 16 h. Cells were then stained with Viability Dye eFluor 780 and Fc block prior to surface staining with mAbs specific for CD4, and CD8. Following staining for surface markers, cells were fixed and permeabilized with BDCytoFix/CytoPerm solution, and intracellular staining performed with mAbs specific for the following proteins, diluted in permeabilization buffer: CD154, IFNγ, IL-2, IL-4, TNF-α, CD3. Cells were washed, resuspended in 2% fetal bovine serum (FBS)/ phosphate buffered

FDA-CBER-2021-5683-0708879

saline (PBS) buffer and acquired on a LSR Fortessa. Data were analyzed by FlowJo (10.4.1). Cytokine-expressing cells were gated within the CD154+ CD4+ T cells and CD69+ CD8+ T cells. Results shown are background (media-DMSO) subtracted.

2.6.2.12.8. Quantitative RT-PCR for Detection of SARS-CoV-2 Viral RNA

For quantification of SARS-CoV-2 virus in nonhuman primate challenge model swabs and bronchoalveolar lavage (BAL) specimens, the US Centers for Disease Control-developed 2019-nCoV_N1 assay, a sensitive reverse transcription-polymerase chain reaction (RT-PCR)-based assay that detects both viral genomic RNA and RNA transcripts, was used (Singh et al, 2020).

2.6.2.12.9. Lung Radiographs and Computed Tomography Scans

Lung radiographs (X-rays) and computed tomography (CT) scans were performed under anesthesia as previously described (Singh et al, 2020; Kaushal et al, 2015). For radiographic imaging, 3-view thoracic radiographs (ventrodorsal, right and left lateral) were obtained one week prior to challenge, and post-challenge on Days 1, 3, 6 and end of project (Day 7/8) or Day 10. High-resolution CT was performed one week prior to challenge and post-challenge on Days 3 and 6, for BNT162b2-immunized and control NHP and end of project (Day 7/8) or Day 10 for all groups. The animals were anesthetized using Telazol (2-6 mg/kg) and maintained by inhaled isoflurane delivered through a Hallowell 2002 ventilator anesthesia system (Hallowell, Pittsfield, MA). Animals were intubated to perform end inspiratory breath-hold using a remote breath-hold switch. Lung field CT images were acquired using Multiscan LFER150 PET/CT (MEDISO Inc., Budapest, Hungary) scanner. Image analysis was performed using 3D ROI tools available in Vivoquant (Invicro, Boston, MA). Images were interpreted by two board-certified veterinary radiologists blinded to treatment groups. Scores were assigned to a total of 7 lung regions on a severity scale of 0-3 per region, with a maximum severity score of 21. Pulmonary lesions that could not be unequivocally attributed to the viral challenge (such as atelectasis secondary to recumbency and anesthesia) received a score of "0".

2.6.2.12.10. Macroscopic and Microscopic Pathology

Histopathological assessments were performed at Days 7 or 8 following infectious SARS-CoV-2 challenge on the BNT162b2-immunized animals (100 µg dose level; n =6) and age- and sex-matched saline-immunized and SARS-CoV-2-challenged control animals that were included in the histopathology animal cohort (n=3). Tissues collected and microscopically evaluated included lung (7 sections- 1 sample of each lobe on L & R), kidney, liver, spleen, skin, large and small intestine, heart [with coronary arteries], bone marrow, nasal septum, tongue, trachea, mediastinal lymph node, and mucocutaneous junctions. Tissues were fixed in 10% neutral buffered formalin and routinely processed into paraffin blocks, sectioned to 5 µm and stained with hematoxylin and eosin.

Microscopic evaluation was performed independently by two pathologists, both blinded to treatment group. Lungs were evaluated using a semi-quantitative scoring system with inclusion of cell types and/or distribution as appropriate. An inflammation area score, based on the estimated area of the lung section with inflammation, was used to grade each lung lobe: 0=normal; 1=<10%; 2=11-30%; 3=30-60%; 4= 60-80%; 5=>80%. Samples were

FDA-CBER-2021-5683-0708880

unblinded after agreement on diagnoses and severity grades. For each animal, the inflammation area score for each lung lobe was averaged to generate a single inflammation area score for that animal. That score was used to evaluate the severity of respiratory disease after SARS-CoV-2 challenge.

2.6.2.13. References

Al-Amri SS, Abbas AT, Siddiq LA, et al. Immunogenicity of candidate MERS-CoV DNA vaccines based on the spike protein. Sci Rep 2017;7:44875.

Baum A, Fulton BO, Wloga E, et al. Antibody cocktail to SARS-CoV-2 spike protein prevents rapid mutational escape seen with individual antibodies. Science 2020; First release

Berger Rentsch M, Zimmer G. A vesicular stomatitis virus replicon-based bioassay for the rapid and sensitive determination of multi-species type I interferon. PLoS One 2011; 6(10):e25858.

Bestle D, Heindl MR, Limburg H, et al. TMPRSS2 and furin are both essential for proteolytic activation and spread of SARS-CoV-2 in human airway epithelial cells and provide promising drug targets. Available from: https://doi.org/10.1101/2020.04.15.042085. Accessed: 24 Sep 2020.

Brouwer PJM, Caniels T G, van der Straten KJ. Potent neutralizing antibodies from COVID-19 patients define multiple targets of vulnerability. Science 2020;369(6504):643-650.

Cai Y, Zhang J, Xiao T, et al. Distinct conformational states of SARS-CoV-2 spike protein. Science 2020:10.1126/science.abd4251.

de Wit E, van Doremalen N, Falzarano D, et al. SARS and MERS: recent insights into emerging coronaviruses. Nat Rev Microbiol 2016;14(8)(08):523-34.

Henderson R, Edwards RJ, Mansouri K, et al. Controlling the SARS-CoV-2 spike glycoprotein conformation. Nat Struct Mol Biol 2020;(Jul):Online.

Hoffmann M, Kleine-Weber H, Schroeder S, et al. SARS-CoV-2 cell entry depends on ACE2 and TMPRSS2 and is blocked by a clinically proven protease inhibitor. Cell 2020; 181(2):271-280.e8.

Hulswit RJ, de Haan CA, Bosch BJ. Coronavirus spike protein and tropism changes. Adv Virus Res 2016;96:29-57.

Hutloff A. Regulation of T follicular helper cells by ICOS. Oncotarget 2015;6(26)(Sep):21785-6.

Kariko K, Buckstein M, Ni H, et al. Suppression of RNA recognition by Toll-like receptors: the impact of nucleoside modification and the evolutionary origin of RNA. Immunity 2005;2(Aug):165-75.

Kaushal D, Foreman TW, Gautam US, et al. Mucosal vaccination with attenuated Mycobacterium tuberculosis induces strong central memory responses and protects against tuberculosis. Nat Commun 2015; 6:8533.

FDA-CBER-2021-5683-0708882

Ke Z, Oton J, Qu K. et al. Structures, conformations and distributions of SARS-CoV-2 spike protein trimers on intact virions. Nature 2020;10.1038/s41586-020-2665-2.

Kim JY, Ko JH, Kim Y, et al. Viral load kinetics of SARS-CoV-2 infection in first two patients in Korea. J Korean Med Sci 2020;35(7)(Feb):e86.

Liu L, Wang P, Nair MS, et al. Potent neutralizing antibodies against multiple epitopes on SARS-CoV-2 spike. Nature 2020;584(7821):450-456.

Munster VJ, Feldmann F, Williamson BN, et al. Respiratory disease and virus shedding in rhesus macaques inoculated with SARS-CoV-2. Available from: https://doi.org/10.1101/2020.03.21.001628. Accessed: 24 Sep 2020.

Muruato AE, Fontes-Garfias CR, Ren P, et al. A high-throughput neutralizing antibody assay for COVID-19 diagnosis and vaccine evaluation. Nat Commun 2020;11(1):4059.

Pallesen J, Wang N, Corbett KS, et al. Immunogenicity and structures of a rationally designed prefusion MERS-CoV spike antigen. Proc Natl Acad Sci USA 2017;114(35):E7348-57.

Pardi N, Parkhouse K, Kirkpatrick E, et al. Nucleoside-modified mRNA immunization elicits influenza virus hemagglutinin stalk-specific antibodies. Nat Commun 2018;9(1)(08):3361.

Report R-20-0085: Immunogenicity Study of the LNP-Formulated ModRNA Encoding the Viral S Protein-V9.

Robbiani DF, Gaebler C, Muecksch F, et al. Convergent Antibody Responses to SARS-CoV-2 Infection in Convalescent Individuals. Available from: https://doi.org/10.1101/2020.05.13.092619. Accessed: 24 Sep 2020.

Sahin U, Karikó K, Türeci Ö. mRNA-based therapeutics - developing a new class of drugs. Nat Rev Drug Discov 2014;13(10):759-80.

Singh DK, Ganatra SR, Singh B, et al. SARS-CoV-2 infection leads to acute infection with dynamic cellular and inflammatory flux in the lung that varies across nonhuman primate species. Available from: https://doi.org/10.1101/2020.06.05.136481. Accessed: 24 Sep 2020.

Slansky JE, Rattis FM, Boyd LF, et al. Enhanced antigen-specific antitumor immunity with altered peptide ligands that stabilize the MHC-peptide-TCR complex. Immunity 2000; 13(4):529-38.

Study 38166. Repeat-Dose Toxicity Study of Three LNP-Formulated RNA Platforms Encoding for Viral Proteins By Repeated Intramuscular Administration to Wistar Han Rats.

Study 20GR142. Giovanelli M. 17-Day Intramuscular Toxicity Study of BNT162B2 (V9) and BNT162B3C in Wistar Han Rats with a 3-Week Recovery. Study ongoing.

FDA-CBER-2021-5683-0708883

Study 20256434 (RN9391R58). Bouressam M. A Combined Fertility and Developmental Study (Including Teratogenicity and Postnatal Investigations) of BNT162b1, BNT162b2 and BNT162b3 by Intramuscular Administration in the Wistar Rat. 22 Dec 2020.

VR-MQR-10211 Method Qualification Report for a Single-Plex Direct Luminex Assay for Quantitation of IgG Antibodies to SARS-CoV-2 S1 Protein in Human Sera.

VR-MQR-10214 neut assay Qualification of the SARS-CoV-2 mNeonGreen Virus Microneutralization Assay.

VR-VTR-10671 BNT162b2 (V9) Immunogenicity and Evaluation of Protection against SARS-CoV-2 Challenge in Rhesus Macaques.

World Health Organization. WHO guidelines on nonclinical evaluation of vaccines. Annex 1. In: World Health Organization. WHO technical report series, no. 927. Geneva, Switzerland; World Health Organization; 2005:31-63.

Wrapp D, Wang N, Corbett KS, et al. Cryo-EM structure of the 2019-nCoV spike in the prefusion conformation. Science 2020;367(6483):1260-3.

Wu Y, Wang F, Shen C, et al. A noncompeting pair of human neutralizing antibodies block COVID-19 virus binding to its receptor ACE2. Science 2020; 368(6496):1274-8.

Xie X, Muruato A, Lokugamage KG, et al. An infectious cDNA clone of SARS-CoV-2. Cell Host Microbe 2020; 27(5):841-848.e3.

Yong CY, Ong HK, Yeap SK, et al. Recent advances in the vaccine development against middle east respiratory syndrome-coronavirus. Front Microbiol 2019;10:1781.

Yuan M, Wu NC, Zhu X, et al. A highly conserved cryptic epitope in the receptor binding domains of SARS-CoV-2 and SARS-CoV. Science 2020; 368(6491):630-3.

Zakhartchouk AN, Sharon C, Satkunarajah M, et al. Immunogenicity of a receptor-binding domain of SARS coronavirus spike protein in mice: implications for a subunit vaccine. Vaccine 2007;25(1):136-43.

Zhou M, Zhang X, Qu J. Coronavirus disease 2019 (COVID-19): a clinical update. Front Med 2020(Apr):1-10.

Zou L, Ruan F, Huang M, et al. SARS-CoV-2 viral load in upper respiratory specimens of infected patients. N Engl J Med 2020;382(12)(03):1177-9.

090177e1962f80a2\Approved\Approved On: 04-Feb-2021 00:09 (GMT)

FDA-CBER-2021-5683-0708884